CHEMISTRY
A EUROPEAN JOURNAL

DOI: 10.1002/chem.200901943

Stabilization of G-Quadruplex DNA with Platinum(II) Schiff Base Complexes: Luminescent Probe and Down-Regulation of c-*myc* Oncogene Expression

Peng Wu,[a] Dik-Lung Ma,[a] Chung-Hang Leung,[a] Siu-Cheong Yan,[a] Nianyong Zhu,[a] R. Abagyan,[b] and Chi-Ming Che*[a]

Abstract: The interactions of a series of platinum(II) Schiff base complexes with c-*myc* G-quadruplex DNA were studied. Complex [PtL^{1a}] (**1a**; H_2L^{1a} = *N*,*N*′-bis(salicylidene)-4,5-methoxy-1,2-phenylenediamine) can moderately inhibit c-*myc* gene promoter activity in a cell-free system through stabilizing the G-quadruplex structure and can inhibit c-*myc* oncogene expression in cultured cells. The interaction between **1a** and G-quadruplex DNA has been examined by ^{1}H NMR spectroscopy. By using computer-aided structure-based drug design for hit-to-lead optimization, an in silico G-quadruplex DNA model has been constructed for docking-based virtual screening to develop new platinum(II) Schiff base complexes with improved inhibitory activities. Complex [PtL^3] (**3**; H_2L^3 = *N*,*N*′-bis{4-[1-(2-propylpiperidine)oxy]salicylidene}-4,5-methoxy-1,2-phenylenediamine) has been identified with a top score in the virtual screening. This complex was subsequently prepared and experimentally tested in vitro for its ability to stabilize or induce the formation of the c-*myc* G-quadruplex. The inhibitory activity of **3** (IC_{50} = 4.4 μM) is tenfold more than that of **1a**. The interaction between **1a** or **3** with c-*myc* G-quadruplex DNA has been examined by absorption titration, emission titration, molecular modeling, and NMR titration experiments, thus revealing that both **1a** and **3** bind c-*myc* G-quadruplex DNA through an external end-stacking mode at the 3' terminal face of the G-quadruplex. Such binding of G-quadruplex DNA with **3** is accompanied by up to an eightfold increase in the intensity of photoluminescence at λ_{max} = 652 nm. Complex **3** also effectively down-regulated the expression of c-*myc* in human hepatocarcinoma cells.

Keywords: G-quadruplex DNA · luminescent probes · onogenes · platinum · Schiff bases

Introduction

G-quadruplex DNA is putatively present in pivotal genomic regions, such as telomeres, oncogene promoters, and most growth control genes.[1,2] Among many of these promoter quadruplex sequences,[4–8] the human oncogene c-*myc* plays a nontrivial role in many cellular events, and the overexpression of this oncogene is linked to cellular proliferation in malignant tumors.[9] In principle, the transcription of c-*myc* is mainly controlled by the nuclear hypersensitivity element III_1 (NHE III_1), which is upstream of the P1 promoter of c-*myc*.[10–14] Thus, the inhibition of the transcription of c-*myc* by inducing and/or stabilizing G-quadruplex formation is a promising strategy for developing efficacious anticancer therapies. Planar aromatic molecules, such as cationic porphyrins (e.g., TMPyP4 and Se2SAP),[15,16] perylenes,[17] and the natural products telomestatin,[18] quindolines,[19] and berberine,[19] are known to bind to and stabilize G-quadruplex DNA in the NHE III_1 sequence and, in some cases, to suppress c-*myc* transcription in cancer cell lines.

Over the past decades, a number of metal complexes developed by various research groups have been reported to be anticancer and antitumor active.[20,21] Lippard, Che,

[a] Dr. P. Wu, Dr. D.-L. Ma, Dr. C.-H. Leung, Dr. S.-C. Yan, Dr. N. Zhu, Prof. Dr. C.-M. Che
Department of Chemistry and Open Laboratory of Chemical Biology
Institute of Molecular Technology for Drug Discovery and Synthesis
The University of Hong Kong, Pokfulam Road, Hong Kong (China)
Fax: (+852) 2857-1586
E-mail: cmche@hku.hk

[b] Prof. R. Abagyan
Skaggs School of Pharmacy & Pharmaceutical Sciences
University of California, San Diego
9500 Gilman Drive, MC 0747 La Jolla, CA 92037-0747 (USA)

Supporting information for this article is available on the WWW under http://dx.doi.org/10.1002/chem.200901943.

McMillin, Lowe, and others have demonstrated that both $[Pt(terpy)X]^+$ (terpy = 2,2′:6′,2″-terpyridine; X = Cl, SR) and $[Pt(terpy)L]^{n+}$ (L = anionic ligand, $n=1$; L = neutral ligand, $n=2$) can bind to DNA and that some of these complexes display promising anticancer properties.[22] Barton and co-workers pioneered the studies on the interactions of DNA with octahedral d^6 metal complexes, such as complexes of ruthenium(II) and rhodium(III). By the judicious choice of auxiliary ligands, octahedral d^6 metal complexes can be developed into good metallointercalators of double-stranded DNA.[23] Despite extensive work on the interactions of metal complexes with helical DNA duplexes, related studies with higher-order secondary DNA structures are still in the rudimentary stages.[24] A manganese(III) porphyrin developed by Pratviel and co-workers bound G-quadruplex DNA with 10000-fold selectivity over duplex DNA and inhibited telomerase with IC_{50} = 580 nM.[24i] Neidle and co-workers reported that square-planar nickel(II) salphen (H_2salphen = *N*,*N*′-bis(salicylidene)-1,2-phenylenediamne) complexes act as potent telomerase inhibitors through the stabilization of G-quadruplex DNA.[24e,n] In view of these findings, we conceive that platinum(II) complexes with Schiff base ligands can be used in the design of G-quadruplex DNA binders for the inhibition of c-*myc* transcription activity because 1) the Pt^{II} ion is substitutionally inert and hence its complexes are kinetically more stable in solution, 2) the planar coordination geometry of a Pt^{II} center together with the use of π-conjugated Schiff base ligands would lead to compounds that stack on the face of guanine quartet of the G-quadruplex, 3) Schiff base ligands are easily structurally modified, and 4) the Pt^{II} cation can locate in the centre of the quartet (i.e., the surface of the G-quadruplex ion channel). Also, platinum(II) complexes containing π-conjugated ligands usually display photoluminescence properties that can be strongly affected by subtle changes in their local environment and can therefore be applied to develop luminescent probes for G-quadruplex DNA in the P1 promoter of c-*myc*.

In this context, we employed the polymerase stop assay and reverse transcriptase-polymerase chain reaction (RT-PCR) assay of c-*myc* expression for the initial screening of platinum(II) Schiff base complexes that may stabilize G-quadruplex DNA. Among the complexes examined, [PtL^{1a}] (**1a**; H_2L^{1a} = *N*,*N*′-bis(salicylidene)-4,5-methoxy-1,2-phenylenediamine; Scheme 1) moderately inhibited c-*myc* gene promoter activity in a cell-free system through stabilizing c-*myc* G-quadruplex DNA and inhibited c-*myc* expression in cultured cells. Thus, this platinum(II) complex was a vital initial lead for optimization through docking-based virtual screening to develop new platinum(II) salphen complexes with improved inhibitory activities. To develop a high-throughput screening platform for compounds that bind to G-quadruplex DNA, a model of the intramolecular G-quadruplex loop isomer of NHE III_1 was constructed by using the X-ray

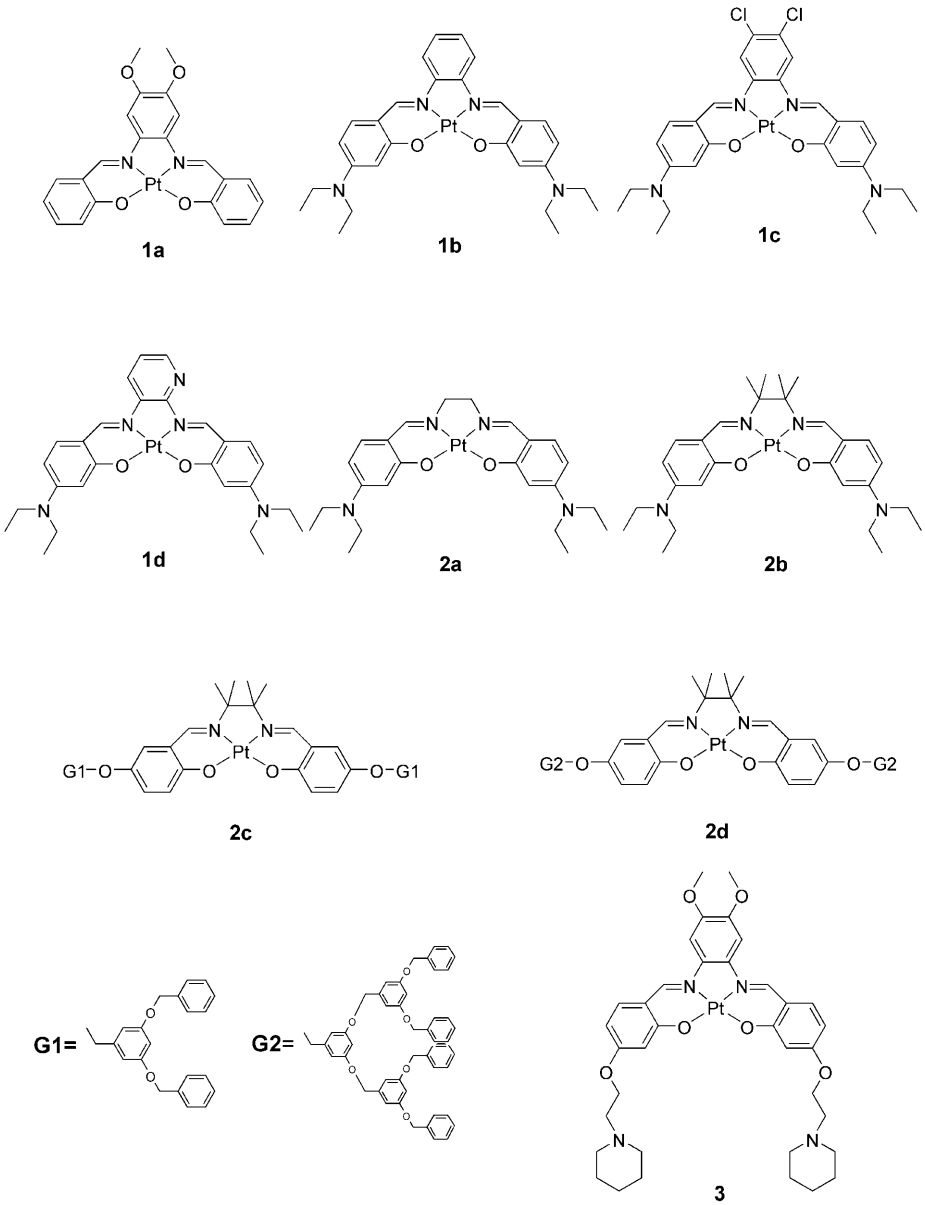

Scheme 1. Structures of complexes **1**–**3**.

crystal structure of the intramolecular human telomeric G-quadruplex DNA (Protein Data Bank (PDB) code: 1KF1).[25] The aforementioned intramolecular G-quadruplex loop isomer model of NHE III_1 has previously been utilized to reveal quindoline complexes to have a salutary effect on stabilizing the G-quadruplex structure in c-*myc*.[19] We report herein that the platinum(II) salphen complex with amine side chains at the periphery of Schiff base ligand **3** is one of the top-scoring complexes found through in silico virtual-ligand screening. Even at micromolar concentrations, this ligand can stabilize or induce G-quadruplex formation and down-regulate c-*myc* in HepG2 cancer cells through inhibition of c-*myc* transcription.

Results

The Schiff base ligands were prepared according to previous reports (see the Experimental Section). The reactions of 1,2-diamine with substituted salicylaldehydes in ethanol gave salphen or *N*,*N*′-bis(salicylidene)ethylenediaminato (salen) ligands, which were recrystallized from ethanol. Treatment of K_2PtCl_4 with Schiff base ligands in acetonitrile (with dimethyl sulfoxide (DMSO)) followed by subsequent purification gave complexes **1**–**3** (see Scheme S1 in the Supporting Information). The structure of **1c** was established by an X-ray crystallographic study (Figure 1). The bond angles and

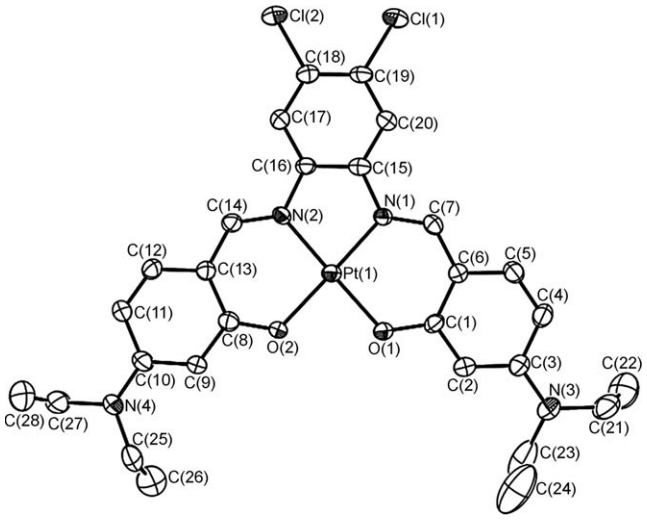

Figure 1. X-ray crystal structure of **1c**.

distances are comparable to those reported for other platinum(II) Schiff base complexes.[26b] Based on UV/Vis absorption and NMR spectroscopic measurements, the platinum(II) Schiff base complexes are stable in aqueous solutions for 72 h at room temperature.

Spectroscopic properties: The UV/Vis absorption spectrum of **3** in CH_2Cl_2 shows two intense absorption bands at $\lambda_{max}=$ 372 and 390 nm ($\varepsilon\approx4.8\times10^4$ and 3.3×10^4 $mol^{-1}dm^3cm^{-1}$, respectively). A moderately intense band is observed at $\lambda_{max}=$ 482 nm ($\varepsilon\approx1.7\times10^4$ $mol^{-1}dm^3cm^{-1}$), with a shoulder at $\lambda_{max}=520$ nm (see Figure S1 in the Supporting Information). According to previous reports,[26a–d] the absorption bands at $\lambda=372$–390 nm are assigned to intraligand transition(s) (ILs), in which the band at $\lambda=482$ nm is assigned to mixed metal-to-ligand charge-transfer (^{1}MLCT) [$Pt(d^5)\rightarrow\pi^*$-(salphen)] and ligand-to-ligand charge-transfer (^{1}LLCT) [(phenoxide)$\rightarrow\pi^*$(imine)] transitions. The absorption spectra of complexes **1a**–**d** and **2a**–**d** are similar to that of **3** in the spectral region $\lambda=280$–400 nm, and all these complexes display intense absorption bands between $\lambda=400$ and 500 nm (see Figures S2–S9 in the Supporting Information).

The absorption spectra of **1**–**3** are sensitive to the solvent. For example, the absorption maximum of **1a** in CH_2Cl_2 is similar to that in CH_3CN ($\lambda_{max}=370$ and 363 nm, respectively), but the lower-energy broad absorption band (and the shoulder (sh) in particular) is red-shifted to low energy in low-polarity solvents; for example, $\lambda_{max}=487$ (518 (sh)), 488 (525 (sh)), 495 (538 (sh)), 497 (550 (sh)) nm in MeOH, CH_3CN, CH_2Cl_2, and benzene, respectively. Such negative solvatochromic shifts reveal that the ground state is more polar than the excited state. This phenomenon has been reported for related platinum(II) Schiff base complexes such as [Pt(8-quinolinol)$_2$].[26e,f] The UV/Vis absorption spectra of **1a** (20 μM) in various solvents are given in the Supporting Information (Figure S2) and the UV/Vis absorption data of **1**–**3** are summarized in Table 1.

Excitation of **3** (50 μM in CH_3CN) at $\lambda=372$ nm gives an emission at $\lambda_{max}=626$ nm (see Figure S10 in the Supporting Information). Emission lifetimes are $\tau=1.40$–4.60 μs and emission quantum yields are around $\phi=0.01$ in CH_3CN. The emission maxima of complexes **1a**–**d** in CH_3CN are at $\lambda_{max}=$ 638 ($\phi=0.05$, $\tau=1.90$ μs), 600 ($\phi=0.22$, $\tau=5.60$ μs), 606 ($\phi=0.10$, $\tau=4.30$ μs), and 595 nm ($\phi=0.13$, $\tau=6.60$ μs), respectively. Complexes **2a**,**b** in CH_3CN display emission maxima at $\lambda_{max}=536$ ($\phi=0.13$, $\tau=3.10$ μs) and 522 nm ($\phi=$ 0.25, $\tau=7.60$ μs), respectively (see Figures S11–S18 in the Supporting Information). Complexes **2c**,**d** are weakly emissive in CH_3CN or CH_2Cl_2. When compared with absorption data, the emission maxima of **1**–**3** are less sensitive to solvent effects. For example, the emission maximum of **3** shifts slightly from $\lambda_{max}=626$ nm in CH_3CN to $\lambda_{max}=628$ nm in CH_2Cl_2 (see Figure S10 in the Supporting Information). The photophysical data of **1**–**3** are summarized in Table 1.

Polymerase stop assay: The induction and/or stabilization of a biologically relevant G-quadruplex by complexes **1** and **2** were examined.[16,18,19a,27] It has been reported that G4A1 oligomer (5′-TGGGGAGGGTGGGGAGGGTGGGGAAGG-3′) could form an intramolecular G-quadruplex structure in the presence of 100 mM KCl. A polymerase stop assay can evaluate the stabilization of intramolecular G-quadruplex structures in the presence of platinum(II) Schiff base complexes. The formation of a G-quadruplex structure would prohibit DNA hybridization and the subsequent polymerase chain reaction (PCR). The relative binding affinities

Table 1. Photophysical data of **1**–**3** in various solvents at 298 K.[a]

Complex	Medium	T [K]	λ_{abs} [nm] (ε [$\times 10^4$ mol^{-1} dm^3 cm^{-1}])	$\lambda_{em(max)}$ [nm] (τ [μs]; Φ_{em})
1a	C_6H_6	298	321 (1.7), 370 (3.6), 392 (4.3), 497 (1.1), 550 (0.9)	639 (2.3; 0.07)
	CH_2Cl_2	298	320 (1.8), 370 (3.8), 386 (4.2), 495 (1.0), 538 (0.8)	639 (2.1; 0.06)
	MeCN	298	316 (1.6), 363 (3.1), 379 (3.4), 488 (0.5), 525 (sh, 0.6)	638 (1.9; 0.05)
	MeOH	298	315 (1.3), 362 (2.4), 379 (2.6), 487 (0.7), 518 (sh, 0.6)	638 (1.4; 0.03)
1b	C_6H_6	298	340 (1.5), 388 (3.3), 403 (2.9), 460 (4.7), 491 (5.3),	600 (7.7; 0.31)
	CH_2Cl_2	298	336 (1.3), 387 (3.3), 405 (3.4), 459 (5.0), 489 (6.1)	600 (6.1; 0.23)
	MeCN	298	331 (1.1), 383 (2.9), 397 (2.9), 453 (4.2), 482 (5.0)	600 (5.6; 0.22)
	MeOH	298	329 (1.1), 383 (3.3), 398 (3.5), 455 (5.0), 482 (5.8)	600 (4.8; 0.16)
1c	C_6H_6	298	351 (1.4), 402 (2.5), 425 (2.9), 469 (4.1), 500 (5.2)	608 (7.6; 0.21)
	CH_2Cl_2	298	346 (1.0), 402 (2.0, sh), 424 (2.6), 469 (3.3), 500 (4.4)	608 (5.4; 0.15)
	MeCN	298	341 (1.0), 400 (2.3, sh), 417 (2.8), 463 (3.6), 491 (4.7)	606 (4.3; 0.10)
	MeOH	298	339 (1.0), 398 (2.4, sh), 417 (2.9), 463 (3.8), 491 (4.7)	605 (4.4; 0.10)
1d	C_6H_6	298	350 (1.0), 425 (2.0), 464 (2.8), 493 (3.5)	596 (7.5; 0.21)
	CH_2Cl_2	298	345(0.8), 425 (2.0), 463 (2.7), 493 (3.5)	596 (6.9; 0.20)
	MeCN	298	340 (0.9), 419 (2.1), 458 (2.9), 487 (3.5)	595 (6.6; 0.13)
2a	C_6H_6	298	288 (1.4), 364 (3.2), 380 (1.7, sh), 488 (0.01, sh)	543 (3.3; 0.16)
	CH_2Cl_2	298	285 (1.2), 359 (2.9), 382 (1.6, sh), 486 (0.01, sh)	542 (3.1; 0.15)
	MeCN	298	285 (0.8), 347 (3.0), 388 (0.95, sh), 478 (0.01, sh)	536 (3.1; 0.13)
	MeOH/CH_2Cl_2 (10:1)	298	282 (0.75), 345 (3.1), 395 (1.0, sh), 478 (0.01, sh)	535 (3.0; 0.13)
2b	C_6H_6	298	345 (0.6, sh), 373 (1.1), 406 (0.4), 485 (0.01, sh)	531 (8.1; 0.32)
	CH_2Cl_2	298	343 (0.6), 367 (1.1), 399 (0.5, sh), 487 (0.01, sh)	523 (8.0; 0.30)
	MeCN	298	340 (0.6, sh), 361 (1.0), 395 (0.7, sh), 488 (0.01, sh)	522 (7.6; 0.25)
	MeOH	298	339 (0.6), 363 (0.82), 394 (0.5, sh), 485 (0.01, sh)	521 (6.9; 0.22)
2c	C_6H_6	298	306 (0.4), 322 (0.40, sh), 426 (0.24), 488 (0.03)	576 (6.2; 0.08)
	CH_2Cl_2	298	304 (0.4), 315 (0.4, sh), 424 (0.23), 486 (0.02)	575 (6.1; 0.08)
	MeCN	298	304 (0.4), 310 (0.4, sh), 421 (0.21), 485 (0.02)	571 (6.0; 0.08)
	MeOH/CH_2Cl_2 (10:1)	298	295 (0.4), 309 (04, sh), 417 (0.28), 485 (0.01)	568 (6.0; 0.07)
2d	C_6H_6	298	287 (1.5), 341 (0.43, sh), 427 (0.22), 489 (0.02)	577 (6.2; 0.08)
	CH_2Cl_2	298	280 (1.7), 341 (0.51, sh), 426 (0.31), 489 (0.02)	576 (6.0; 0.08)
	MeCN	298	277 (1.7), 338 (0.52, sh), 421 (0.30), 488 (0.03)	574 (4.7; 0.07)
	MeOH/CH_2Cl_2 (10:1)	298	275 (1.1), 332 (0.38, sh), 417 (0.23), 488 (0.03)	573 (4.2, 0.07)
3	CH_2Cl_2	298	314 (1.9), 328 (1.8), 372 (4.8), 390 (3.3), 453 (1.7), 482 (1.7)	628 (4.6; 0.01)
	MeCN	298	309 (1.9), 324 (1.8), 369 (3.3), 383 (3.0), 448 (1.6), 476 (1.6)	626 (3.1; 0.01)
	MeOH	298	309 (1.9) 324 (1.8), 368 (3.1), 383 (2.9), 446 (1.6), 474 (1.5)	626 (1.4; <0.01)
	C_6H_6	298	n.d.	n.d.

[a] n.d. = not determined due to poor solubility; sh = shoulder.

of the platinum(II) complexes to the intramolecular G-quadruplex structure were determined by incubating fixed concentrations of each platinum(II) complex with a DNA template containing the G4A1 c-*myc* sequence in the presence of Taq polymerase. In the presence of a platinum(II) Schiff base complex, the single-stranded G4A1 sequence could be induced into a G-quadruplex structure that blocked hybridization with a complementary strand overlapping the last G repeat. Also, introduction of the platinum(II) complex could stabilize the preformed G4A1-quadruplex structure. In either case, PCR would be inhibited, and the final 43-base pair (bp) double-stranded DNA PCR product would not be detected. The addition of complexes **1a**–**d** and **2a**,**b** at a concentration of 50 μM resulted in a decrease in the intensity of the band that corresponds to the 43-bp double-stranded PCR product in all cases. The highest decrease in the formation of the PCR product was attained with complexes **1a**–**d** (Figure 2). The induction or stabilization of G4A1 G-quadruplex formation by **2c**,**d** could not be determined due to their low solubility in buffer solution.

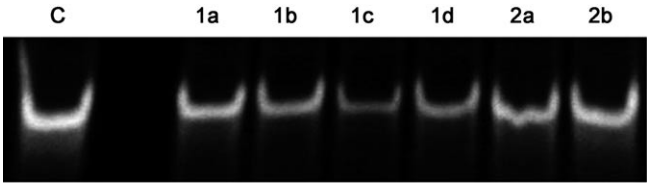

Figure 2. Effect of **1** and **2** (50 μM) on G4A1 G-quadruplex stabilization by the polymerase stop assay.

To confirm the impact of platinum(II) Schiff base complexes on G4A1 G-quadruplex stabilization, a parallel experiment that used oligomer G4A2 (5′-TGGGGAGGGTGGAAAGGGTGGGGAAGG-3′) was performed. The G4A2 sequence is unable to form a G-quadruplex structure, and no inhibition was observed under the same reaction conditions.

Inhibition of the expression of c-*myc* in cancer cells: To evaluate the ability of platinum(II) Schiff base complexes to inhibit c-*myc* transcription in cancer cells, RT-PCR assays were performed.[19a] Complex **1a** was the strongest inhibitor of c-*myc* expression. At a concentration of 50 μM, this complex significantly decreased the mRNA level of c-*myc* in HepG2 cells (human hepatocarcinoma; Figure 3). This

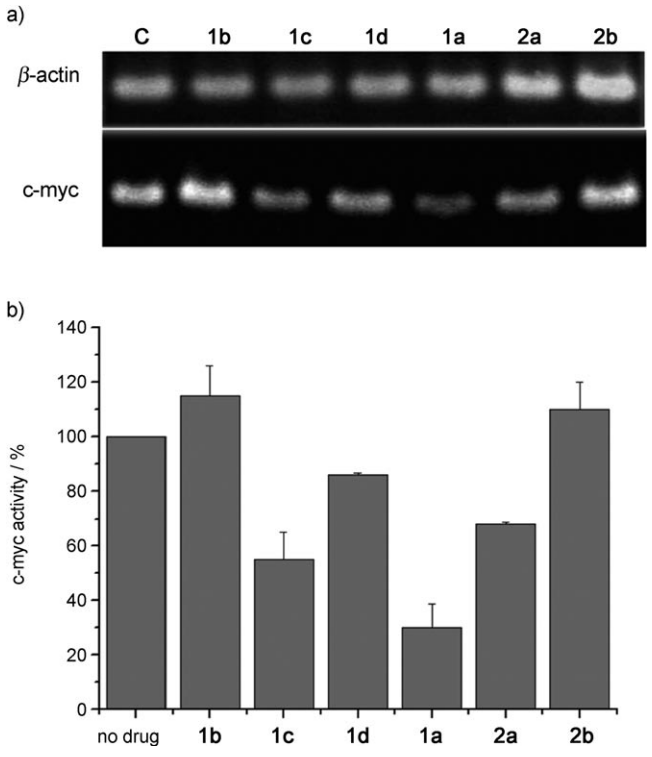

Figure 3. a) Expression of c-*myc* in HepG2 cells treated with **1** and **2** by RT-PCR. b) Percentage of c-*myc* activity for **1** and **2**.

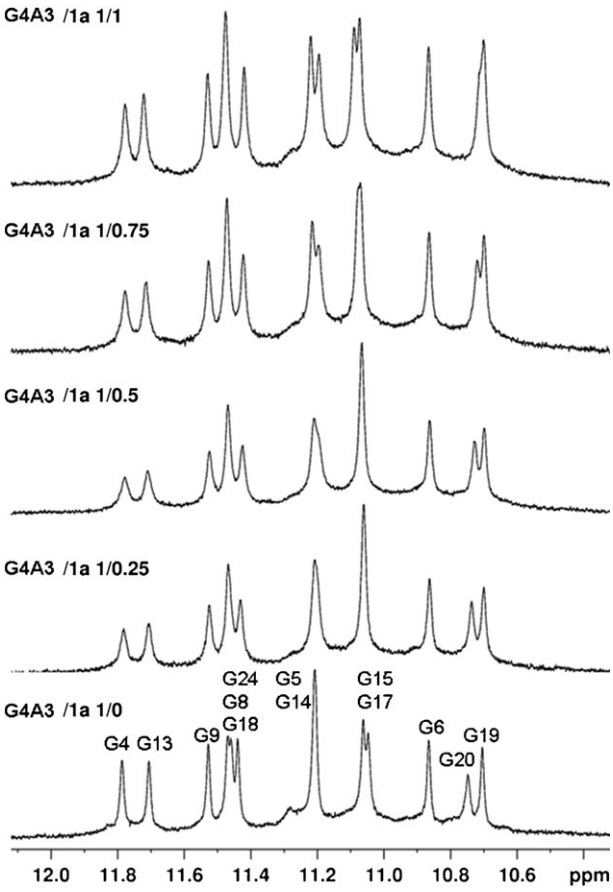

Figure 4. NMR titration (600 MHz, 27 °C) of the intramolecular G4A3 quadruplex with **1a** at various ratios of [**1a**]/[G4A3 quadruplex] in H_2O/D_2O (90:10) with KCl (150 mM), KH_2PO_4 (25 mM), and EDTA (1 mM; pH 7.0). The imino proton resonances of the residues in the G-tetrad were assigned on the basis of previous data.[28]

result suggests that **1a** can suppress the transcription of c-*myc* through interaction with the NHE III_1 upstream of the P1 promoter of c-*myc*. Because **1a** was the most potent complex against c-*myc* transcription, it was used in subsequent studies to elucidate the interaction between platinum(II) Schiff base complexes and the G-quadruplex.

NMR spectroscopic experiments: To elucidate the binding mode of **1a**, we conducted a number of ^{1}H NMR spectroscopic experiments in phosphate buffer solution (H_2O/D_2O (90:10) with KCl (150 mM), KH_2PO_4 (25 mM), and ethylenediaminetetraacetic acid (EDTA; 1 mM), pH 7.0). An intramolecular G4A3 quadruplex[28] (5′-TGAGGGTGGIGAGGGTGGGGAAGG-3′) with clearly assigned G-tetrad imino proton signals[28] was used for these studies. Upon the addition of **1a** to a solution of the G4A3 quadruplex in the phosphate buffer (1.0 mM) to obtain a [**1a**]/[G4A3 quadruplex] ratio of 1:1, the imino proton resonances of the residues in the G-tetrad were shifted upfield (Figure 4). At a ratio of 1:0 for [**1a**]/[G4A3 quadruplex], the G6 and G20 imino proton signals experienced the largest shift, thus revealing that **1a** binds close to the 3' terminal face of the G-quadruplex DNA. The changes in chemical shifts are similar to those displayed by daunomycin, which is known to bind to G-quadruplexes.[28] We favor the model that **1a** binds externally to the stacks of guanine quartets within a quadruplex, rather than intercalating between the stacks.

Molecular modeling: We performed molecular modeling of the binding of **1a** on the model of the NHE III_1 intramolecular G-quadruplex loop isomer to further investigate the mode of binding. Hurley and co-workers showed that the biologically relevant parallel c-*myc* G-quadruplexes can exist as a mixture of four loop isomers (see Figure S19 in the Supporting Information) with predominance of the 1:2:1 and 2:1:1 isomers.[29a] Independent work by Patel and co-workers that employed high-field NMR spectroscopic analysis also showed the predominance of the 1:2:1 loop isomer in the c-*myc* parallel G-quadruplex.[29b] Because neither NMR spectroscopic nor X-ray crystallographic information of the NHE III_1 1:2:1 loop isomer is available, a model was built from the known, closely related X-ray crystal structure of the human intramolecular telomeric G-quadruplex DNA. A truncated 18-bp sequence (i.e., 5′-AGGGTGGGGAGGGTGGGG-3′) was used for this study because nucleotides G2–G5 in the G4A1-c-*myc* sequence 5′-T*GGGG*AGGGTGGGGAGGGTGGGGAAGG-3′ are not involved in the G-quartet structure. The modeling study mirrors the general trend that **1a** binds to the G-quadruplex

with a calculated binding energy of approximately $-50\,kcal\,mol^{-1}$ and is stacked at the ends of G-quadruplex at the GT-quadruplex terminus, close to the 3' terminal face of the G-quadruplex. This model is consistent with that derived from the results of the NMR spectroscopic experiments described in previous section. In addition, the unfavorable binding energies of approximately $+30\,kcal\,mol^{-1}$, calculated for the intercalation binding sites, suggest that the interactions between **1a** and G-quadruplex DNA should not be intercalative in nature (see Table S1 in the Supporting Information). As such, **1a** is an useful scaffold for developing new platinum(II) analogues with improved inhibitory activities against c-*myc* transcription.

Lead optimization: The encouraging results obtained from preliminary screening suggested the use of **1a** as an appropriate starting scaffold for hit-to-lead optimization through virtual screening. To give new lead derivatives with improved potency and specificity against c-*myc* transcription, we adopted a structure-guided parallel synthesis. In this approach, the Schiff base is modified on the basis of receptor structural information, and the mode of binding of the platinum(II) complex with the G-quadruplex DNA serves as a template for lead optimization (Figure 5). Molecular modeling permits rapid screening of multiple analogues, thus facilitating preselection of a subset of furnished analogues with favorable binding affinities. This approach can expedite the discovery of derivatives of **1a** that exhibit greater specificity and selectivity toward the G-quadruplex structure of c-*myc*.

By using the above approach and with **1a** as the structural template, 60 new platinum(II) Schiff base complexes containing different amine side chains were virtually screened (see Figure S20 in the Supporting Information). The top-scoring platinum(II) complex was evaluated for its effect on stabilizing G-quadruplex DNA. The platinum(II) complex was docked to a grid representation of the receptor and a score was assigned to each complex that reflected the quality of the interaction according to the iterated conditional modes (ICM) method (Molsoft).[30] Analysis of the conformational energy of all of the platinum(II) Schiff base complexes revealed that the side chains can bury deeply in the G-quadruplex DNA grooves, thus making several electrostatic and hydrogen-bonding contacts. However, the $n=2$ side chain is generally superior to the $n=1$, 3, 4, and 5 side chains (see Figure S20 in the Supporting Information). The top-scoring molecule identified through virtual screening was [Pt^{II}(*N*,*N*′-bis{4-[1-(2-propylpiperidine)oxy]salicylidene}-4,5-methoxy-1,2-phenylenediamine] (**3**; Figure 6). This complex was subsequently prepared and tested experimentally on its ability to inhibit the amplification in the promoter region of c-*myc* with the polymerase stop assay. Notably, **3** promoted/stabilized the formation of the G-quadruplex to the greatest extent with a tenfold boost in inhibition activity ($IC_{50}=4.4\,\mu M$) over the initial hit complex **1a** (see Figure S21 in the Supporting Information).

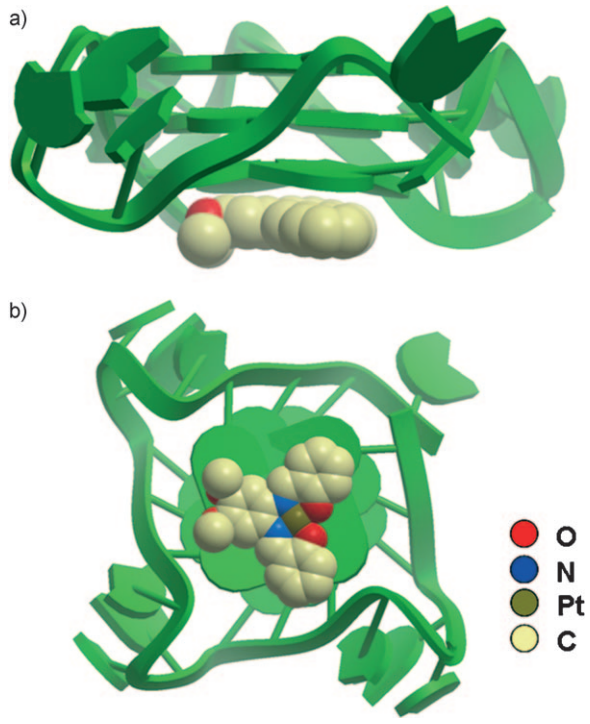

Figure 5. Schematic diagram of the a) side and b) top views of the interactions of **1a** with the G-quadruplex structure of c-*myc*. The G-quadruplex and **1a** are shown in ribbon and space-filling representations, respectively.

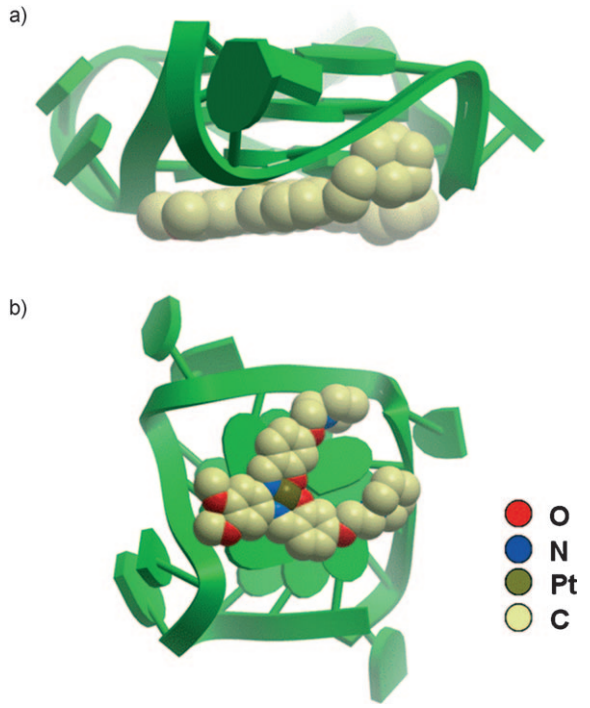

Figure 6. Schematic diagram of the a) side and b) top views of the interactions of **3** with the G-quadruplex structure of c-*myc*. The G-quadruplex and **3** are shown in ribbon and space-filling representations, respectively.

Absorption titration: The ability of the top-scoring complex **3** to interact with the intramolecular G-quadruplex DNA of c-*myc* was studied by absorption titration experiments. An intramolecular G-quadruplex c-*myc* was prepared by incubating a G4A1 oligonucleotide in tris(hydroxymethyl)aminomethane (Tris)/KCl buffer, which was heated to 95 °C for 10 minutes and cooled to room temperature overnight. The expected secondary DNA structure was confirmed by a positive CD peak at $\lambda = 262$ nm and a negative CD peak at approximately $\lambda = 240$ nm. Isosbestic spectral changes and hypochromism effects were observed in the UV/Vis absorption spectral changes (Figure 7). This hypochromic phenomenon is assigned to the strong interaction between the electronic states of the platinum(II) complex and DNA bases. By using the Scatchard equation,[31] the plot of $D/\Delta\varepsilon_{ap}$ versus D (Figure 7, inset) revealed the binding constant K of **3** with the G-quadruplex to be $K = 1.72 \pm 0.26 \times 10^5$ dm^3 mol^{-1} at 20.0 °C. The K values for **1** and **2** were similarly determined to be approximately $K = 10^5$ dm^3 mol^{-1}. To examine the binding specificity, we employed a duplex G4A1 oligonucleotide as a control. Binding of **3** to G-quadruplex DNA is favored by approximately tenfold compared to non-quadruplex double-stranded DNA molecules ($K = 1.91 \pm 1.10 \times 10^4$ dm^3 mol^{-1} for double-stranded DNA).

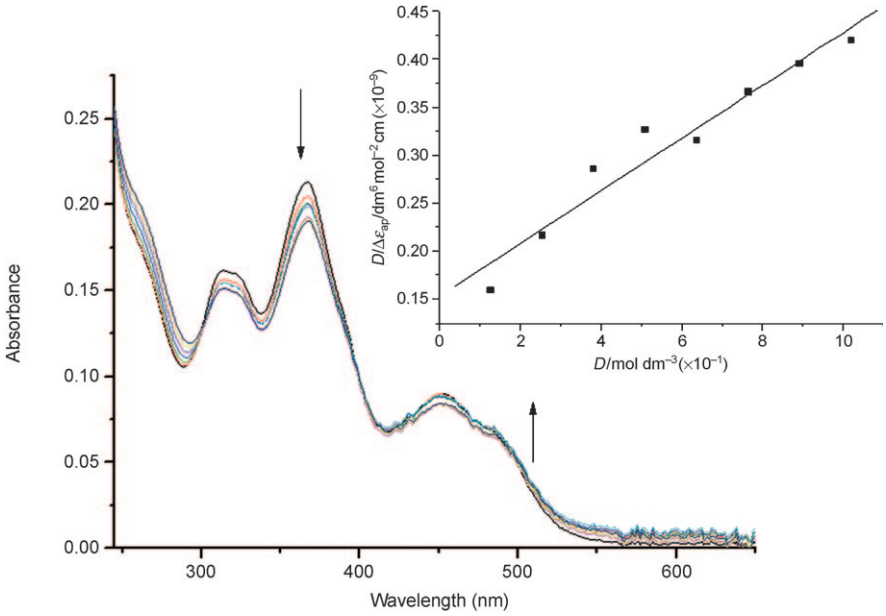

Figure 7. UV/Vis spectra of **3** (25 μM) in Tris/KCl buffer (KCl (100 mM), Tris/HCl (10 mM); pH 7.5) with increasing amount of oligonucleotide G4A1 at 20.0 °C ([G4A1 quadruplex]/[Pt] = 0–20:1). Inset: plot of $D/\Delta\varepsilon_{ap}$ versus D.

Dosage-dependent inhibition of cancer-cell growth and c-*myc* expression: To evaluate the dose response of platinum(II) Schiff base complexes on the inhibition of cancer-cell growth, proliferation assays were performed. By using an MTT assay, the cytotoxicities of **1a**, **1c**, **3**, and cisplatin against HeLa, HepG2, SUNE1, and NCI-H460 cancer-cell lines were determined in vitro, whereas the cytotoxicity toward normal cells was evaluated with the CCD-19Lu normal lung fibroblast cell line. The IC_{50} value of the complexes after incubation for 48 h are on the order: **1a** > **3** ≈ cisplatin ≫ **1c** (Table 2). Notably, the cytotoxicity of **1a** against cancer-cell lines ($IC_{50} = \approx 1$ μM) is approximately tenfold higher than cisplatin. Complex **3** is moderately cytotoxic with IC_{50} values of 8–14 μM. Importantly, this complex is approximately tenfold less cytotoxic ($IC_{50} = 85$ μM) toward normal lung fibroblast cells. The treatment of HepG2 with 25 μM **3** decreased the level of c-*myc* expression (Figure 8). The transcription of c-*myc* is significantly suppressed in the presence of 100 μM **3**. We have thus demonstrated that **3** can down-regulate the expression of c-*myc* at the RNA level in a dose-dependent manner in HepG2 cells.

Emission titration: The design of efficacious luminescent probes for G-quadruplexes is of considerable interest in biochemistry. For this reason, emission titration experiments were conducted to determine the ability of the platinum(II) Schiff base complexes to detect G-quadruplex structures. Complex **3** is weakly emissive in aqueous Tris/KCl buffer solution at 20.0 °C. Upon addition of the G4A1 quadruplex, an intense emission at $\lambda_{max} = 652$ nm is observed (Figure 9). The emission intensity increases with the concentration of the G-quadruplex and is

Table 2. Cytotoxicities of **1a**, **1c**, **3**, and cisplatin toward four carcinoma cell lines.[a]

Complex	IC_{50} [μM]				
	HeLa	HepG2	SUNE-1	NCI-H460	CCD-19 Lu
1a	1.28 ± 0.33	1.09 ± 0.14	1.04 ± 0.21	4.80 ± 0.56	46.11 ± 0.53
1c	86 ± 5.3	> 100	> 100	> 100	> 100
3	12.1 ± 0.43	8.07 ± 0.11	14.04 ± 0.23	11.90 ± 0.26	85.04 ± 0.20
cisplatin	12.5 ± 1.1	11.5 ± 0.12	13.6 ± 0.32	16.5 ± 0.82	85.2 ± 0.36

[a] HeLa = human cervix epithelioid carcinoma, HepG2 = human hepatocellular carcinoma, SUNE-1 = human nasopharyngeal carcinoma, NCI-H460 = human non-small cell lung cancer, and CCD-19Lu = normal human lung fibroblast.

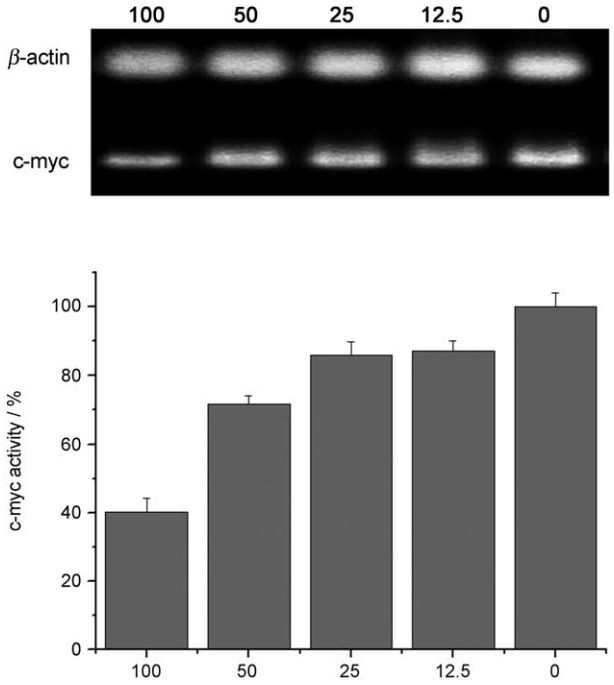

Figure 8. Above: the expression of c-*myc* in HepG2 cells treated with **3** by RT-PCR. Below: percentage of c-*myc* mRNA level (lower panel).

saturated at a [G-quadruplex]/[**3**] ratio of $\geq$20:1. The emission intensity at $\lambda = 652$ nm is enhanced by up to eightfold.

Discussion

Overexpression of the c-*myc* oncogene is linked to increased cellular proliferation and inhibition of differentiation. Thus, c-*myc* is implicated in the development of human and animal malignancies, including carcinomas of the breast, colon, cervix, small-cell lung cancer, osteosarcomas, glioblastomas, and myeloid leukemias.[1–9] Therefore, the inhibition of c-*myc* gene transcription by inducing G-quadruplex formation and/or stabilizing the G-quadruplex structure can be targeted, which can be used in the design of new anticancer therapeutic agents. There have already been reports of organic compounds as telomerase inhibitors that bind to and stabilize G-quadruplexes, thus resulting in the down-regulation of c-*myc*.[17–20] Herein, a class of phosphorescent platinum(II) complexes containing π-conjugated Schiff base ligands with amine side chains were found through computer-aided structure-based drug design. This class of platinum(II) Schiff base complexes are structurally similar to the reported planar organic molecules that are known to bind to G-quadruplexes.

Eight platinum(II) Schiff base complexes were prepared for initial screening to induce and/or stabilize the c-*myc* G-quadruplex structures and inhibit c-*myc* expression by using polymerase stop assays and RT-PCR assays. The platinum(II) complexes **2c**,**d** containing dendritic ligands were prepared for their ability to simultaneously interact with the

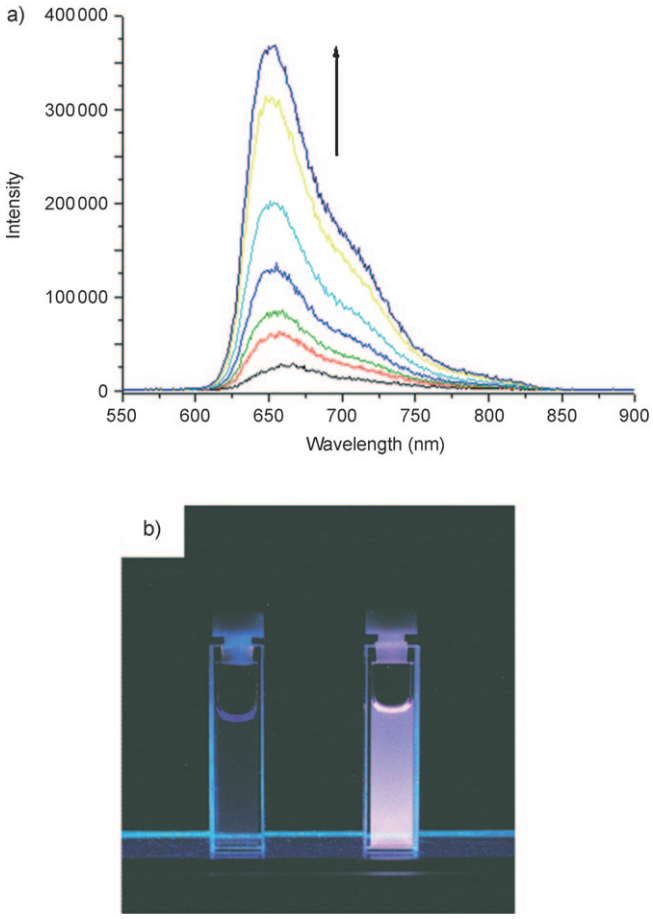

Figure 9. a) Emission spectral traces of **3** (50 μM) in Tris/KCl buffer with increasing concentration of the G-quadruplex at 20.0 °C. b) Photographs of **3** in the absence and the presence of the G-quadruplex.

minor groove of DNA. The work by Smith and co-workers showed that dendritic arrays of spermine ligands with inherent repetitive branded structures offer a useful scaffold for organizing multiple ligands on an accessible surface to achieve high nonspecific minor-groove DNA binding affinity.[32] However, the poor water solubility of complexes **2c**,**d** limits their applications in DNA binding studies.

Based on the results of the initial preliminary screening by using the polymerase stop assay and RT-PCR assay, complex **1a** emerged as an appealing scaffold for optimization through docking-based virtual screening to improve inhibitory activities. Subsequently, we designed and prepared platinum(II) Schiff base complexes with the following characteristics: 1) a rigid flat Schiff base mainframe that promotes π–π stacking for binding to a G-quadruplex and 2) amine side chains attached to the Schiff base ligand for interactions with G-quadruplex loops and grooves.

Specificity for G-quadruplex DNA of the c-*myc* sequence over duplex DNA: We studied the interaction of the platinum(II) Schiff base complexes with the G-quadruplex oligonucleotide from the promoter region of the oncogene c-*myc* by UV/Vis absorption and emission titration experiments.

The results show that the platinum(II) Schiff base complexes can bind to G-qudruplex DNA with binding constants of approximately $K=10^5\,dm^3\,mol^{-1}$. By comparing the K values, complex **3** has a nearly tenfold higher binding affinity toward the intramolecular c-*myc* G-quadruplex DNA from oligonucleotide G4A1 than for non-quadruplex double-stranded DNA molecules consisting of complementary G4A1 oligonucleotides. This significant level of selectivity for c-*myc* G-quadruplex DNA over duplex DNA validates the results of the computer-aided design of the Schiff base ligands with hydrogen-bonding donor/acceptor amine side chains for effective stabilization of G-quadruplex structures.

Hit-to-lead optimization through computer-aided virtual screening: In this study, we identified that complex **3** displays selectivity for the c-*myc* G-quadruplex over double-stranded DNA. Molecular modeling was used to rationalize the selectivity of **3**. Our initial lead complex **1a** was shown to bind to the c-*myc* G-quadruplex, thus leading to inhibition of c-*myc* gene promoter activity and repression of c-*myc* transcription. Computer-aided molecular docking of the interactions of a series of platinum(II) Schiff base complexes with the c-*myc* G-quadruplex revealed that these platinum(II) complexes have optimal stacking interactions at one end of the G-quadruplex structure. The platinum(II) ion in these complexes is positioned at the center of the quartet (i.e., the surface of the G-quadruplex ion channel), which can provide additional electrostatic stabilization. As reported previously, the strength of the interaction between planar π-conjugated molecules and G-quadruplex DNA can be increased considerably by attaching side chains to the planar core of the molecule.[19,20,24e,l] We have examined the effect of the length of the aliphatic spacer on the binding properties of platinum(II) Schiff base complexes by molecular docking. The $n=2$ side chain is generally superior to the $n=$ 1, 3, 4, and 5 side chains (see Figure 6 and Figure S20 in the Supporting Information).

It has been reported that the biologically relevant G-quadruplexes of NHE III_1 exist as a dynamic mixture of four different loop isomers, and all four isomers contribute to the stability of the silencer element in NHE III_1 of the c-*myc* promoter, thus functioning as transcriptional repressor elements. The 1:2:1 form is the major isomer,[29] but because neither NMR spectroscopic nor X-ray crystallographic information is available for the 1:2:1 loop isomer of NHE III_1, the model was built from the known, closely related X-ray crystal structure of the human intramolecular telomeric G-quadruplex DNA as previously described.[19a]

On the basis of NMR titration experiments, we hypothesized that **1a** or **3** binds to this G-quadruplex and is stacked on the ends of the G-quadruplex at the GT-quadruplex terminus, which is close to the 3' terminal face of the G-quadruplex. This proposed model is supported by a molecular modeling study of the binding interaction between **3** and intramolecular G-quadruplex DNA (with a favorable calculated binding energy of $-65.88\,kcal\,mol^{-1}$ (i.e., intramolecular G-quadruplex)). Initially, various orientations of **3** were obtained that differ in orientation of the core with respect to the loops of the quadruplex. The energy of these structures was minimized, and the most stable structure that showed the best interaction energy and optimum interactions between **3** and the G-tetrad was selected. A similar external end-stacking binding mode has also been reported in a recent crystal-structure analysis of disubstituted acridine derivatives and a dimeric *Oxytricha* quadruplex.[33] Neidle and co-workers have reported X-ray fiber diffraction data of the cocomplex formed by interaction of a 1,4-disubstituted amidoanthraquinone (BSU-1071) with a synthetic $[d(TGGGT)]_4$ sequence, thus revealing an external end-stacking binding mode.[34]

In addition, the unfavorable binding energies of approximately 43 $kcal\,mol^{-1}$ calculated for the intercalation binding sites reveal that the interaction between **3** and G-quadruplex DNA is not intercalative in nature. All these results can be rationalized by a molecular modeling study on the interactions of **3** with the intercalation sites of G-quadruplex DNA, thus revealing that the core of molecule **3** and the long side chains are too large for intercalation.

Inhibition of c-*myc* gene promoter activity in a cell-free system and its expression in cultured cells: The specific binding of complexes **1a–d, 2b**, and **3** with intramolecular G-quadruplex structures in the promoter region prevents DNA hybridization and subsequent *Taq* polymerase-mediated DNA extension, the inhibition of which can be used as a measure of the stabilization of G-quadruplex structures. Results from the polymerase stop assays reveal that the concentration-dependent inhibition of DNA amplification by complex **3** is due to stabilization of the G-quadruplex structure formed in the DNA templates containing the G4A1 c-*myc* sequence. For each platinum(II) complex examined, there is significantly greater decrease in the amount of the PCR product upon increasing the concentration of the complex. Complex **3** displays the strongest inhibition ($IC_{50}=$ 4.4 μM) and is of comparable potency to quindoline compounds ($IC_{50}=\approx$6–36 μM) and reported 9-*N*-substituted berberine compounds ($IC_{50}=$2–7.1 μM).[19] Compared to **1a**, complex **3** displayed a tenfold increase in potency toward the c-*myc* G-quadruplex (Figure 3). The most potent c-*myc* G-quadruplex stabilizer that has been reported is Se2SAP, with $IC_{50}=0.03$ μM. However, Se2SAP only moderately inhibits down-regulation of c-*myc* in cancer cells.[16] It is possible that Se2SAP is not taken up into the cells due to its relatively large, expanded porphyrin scaffold.

To verify the observed effects of **3** on the c-*myc* promoter G-quadruplex, we examined whether treatment of HepG2 cells with **3** could interfere with c-*myc* expression. The results indicate that **3** decreases c-*myc* expression at the RNA level in HepG2 cells. In contrast, the initial hit complex **1a** displayed a decreased effect in all of the cell-free and cell-based assays compared with **3**. Complex **3** has an extended π-conjugated planar organic ligand that contains hydrogen-bonding donor/acceptor amine side chains. These amine side

chains are needed for specific G-quadruplex binding, as the Schiff base ligand alone promotes or stabilizes the formation of an intramolecular G-quadruplex to a much lesser extent, as confirmed by the results of the UV/Vis absorption titration experiment and polymerase stop assays.

For G-quadruplex binding molecules to act as c-*myc* oncogene regulators, the former must display a high selectivity for G-quadruplex DNA over duplex DNA and a low inhibition concentration against c-*myc* transcription. Based on the RT-PCR assays, complex **3** decreased the transcription of c-*myc* in HepG2 cells at 25 μM and that transcription was significantly repressed at 100 μM. We also used an MTT assay to determine cytotoxicity against tumor cells and normal cells. Complex **3** displays moderate, but significant, cytotoxicity against cancerous cells (IC_{50} = 8–14 μM) but is tenfold less cytotoxic (IC_{50} = 85 μM) toward normal lung fibroblast cells. This selectivity makes it possible for **3** to effectively inhibit c-*myc* gene promoter activity at concentrations that do not have a significant toxic effect upon normal cells. As an aside, we note that complex **1a** is highly cytotoxic against cancer cells (IC_{50} = 1 μM), whereas the effective concentration needed to inhibit c-*myc* transcription is approximately 50 μM, thus revealing that the primary cellular target of **1a** may not be the c-*myc* G-quadruplex.

Conclusions

In summary, a series of platinum(II) complexes containing Schiff base ligands have been prepared and characterized, including X-ray crystallography studies. One of the platinum(II) Schiff base complexes is a promising initial lead compound that shows selective binding to the c-*myc* promoter G-quadruplex over duplex DNA. This complex was demonstrated to inhibit c-*myc* gene promoter activity in a cell-free system and c-*myc* expression in cultured cells. Subsequent computer-aided hit-to-lead optimization furnished a new platinum(II) Schiff base complex with amine side chains that displays superior c-*myc* regulator properties, presumably through stabilization of the G-quadruplex DNA structure in the NHE III_1 sequence.

Experimental Section

Materials: DNA oligomers (G4A1 = 5′-TGGGGAGGGTGGGGAGGGTGGGGAAGG-3′; G4A2 = 5′-TGGGGAGGGTGGAAAGGGTGGGGAAGG-3′; G4A3 = 5′-TGAGGGTGGIGAGGGTGGGGAAGG-3′; c-*myc* S = 5′-GTTAGCTTCACCAACAGGAACTATG-3′; c-*myc* A = 5′-ATACAGTCCTGGATGATGATGTTTT-3′; β-actin S = 5′-GCGTCTGGACCTGGCTGGCCGGGAC-3’ β-actin A = 5′-AAGGAAGGCTGGAAGAGTGCCTCAG-3′) were obtained from Tech Dragon Limited (Carlsbad, CA). Unless otherwise stated, spectroscopic titration experiments were performed in 10 mM Tris/HCl (pH 7.4) containing 100 mM KCl. SuperScript II Reverse Transcriptase was purchased from Invitrogen (Hong Kong). *Taq* DNA polymerase and the total RNA isolation kit (RNeasy mini kit) were purchased from QIAGEN (Valencia, CA). Stock solutions of all the platinum(II) complexes (10 mM) were made in dimethyl sulfoxide (DMSO) or double-distilled water. Further dilutions to working concentrations were made with double-distilled water.

Physical measurements: Absorption spectra were recorded on a Perkin–Elmer Lambda 19 UV/Vis spectrophotometer. Emission spectra were recorded on a SPEX Fluorolog-2 Model fluorescence spectrophotometer. Positive-ion FAB mass spectra were recorded on a Finnigan MAT95 mass spectrometer.

***N*,*N*′-Bis(salicylidene)-4,5-methoxy-1,2-phenylenediamine (H_2L^{1a})**: Salicylaldehyde (0.4 g, 3.3 mmol) in ethanol (5 mL) was added dropwise to 4,5-dimethoxy-*o*-phenylenediamine (0.22 g, 1.3 mmol) in ethanol (20 mL) at room temperature. The reaction mixture was gradually heated to 60 °C and maintained at this temperature for 4 h. Upon removal of the solvent and cooling, a yellow precipitate was collected and recrystallized from ethanol to give the product (0.2 g, 40 %). ^{1}H NMR ($CDCl_3$, 300 MHz): δ = 13.15 (s, 2H), 8.60 (s, 2H), 7.39–7.35 (m, 4H), 7.05 (d, 2H), 6.94 (d, 2H), 6.80 (s, 2H), 3.97 ppm (s, 6H); MS (FAB, +ve): *m/z*: 376 $[M]^+$.

[PtL^{1a}] (1a): Sodium acetate (0.1 g, 0.27 mmol) was added to H_2L^{1a} (0.1 g, 0.27 mmol) dissolved in MeCN (20 mL), and the solution was stirred for 5 min. K_2PtCl_4 (0.11 g, 0.27 mmol) and DMSO (1 mL) were added to the reaction mixture, which was heated to 40 °C and stirred overnight. After cooling to room temperature, the solvent was removed under vacuum. A yellow precipitate was collected and dissolved in CH_2Cl_2 (10 mL). The organic layer was washed with water (3 × 10 mL), dried over Na_2SO_4, and concentrated to give a red solid (61 mg, 40 %). ^{1}H NMR (CD_3CN, 400 MHz): δ = 8.99 (s, 2H), 7.77 (s, 2H), 7.61 (s, 2H), 7.58 (t, 2H), 7.15 (d, 2H), 6.82 (t, 2H), 3.99 ppm (s, 6H); MS (FAB, +ve): *m/z*: 570 $[M]^+$; elemental analysis calcd (%) for $C_{22}H_{18}N_2O_4Pt$: C 46.40, H 3.19, N 4.92; found: C 46.39, H 3.20, N 4.90.

***N*,*N*′-Bis(4-diethylaminosalicylidene)-1,2-phenylenediamine (H_2L^{1b})**: 4-(Diethylamino)salicylaldehyde (1 g, 5.2 mmol) in ethanol (10 mL) was added dropwise to 1,2-phenylenediamine (0.56 g, 5.2 mmol) in ethanol (40 mL) at room temperature. The mixture was gradually heated to 60 °C and maintained at this temperature for 4 h. Upon removal of the solvent and cooling, a yellow precipitate was collected and recrystallized from ethanol to give the product (1.95 g, 82 %). ^{1}H NMR ($CDCl_3$, 300 MHz): δ = 13.52 (s, 2H), 8.39 (s, 2H), 7.16 (d, 2H), 7.00 (d, 2H), 6.75 (d, 2H), 6.25 (d, 2H), 6.20 (s, 2H), 3.38 (q, 8H), 1.20 ppm (t, 12H); ^{13}C NMR ($CDCl_3$, 300 MHz): δ = 165.0, 161.2, 152.3, 142.8, 134.1, 126.5, 119.6, 109.9, 104.1, 98.6, 45.0, 13.1 ppm; MS (FAB, +ve): *m/z*: 459 $[M]^+$; elemental analysis calcd (%) for $C_{28}H_{34}N_4O_2$: C 73.33, H 7.47, N 12.22; found: C 72.76, H 7.48, N 12.81.

[PtL^{1b}] (1b): Sodium acetate (0.33 g, 4.0 mmol) was added to H_2L^{1b} (1.0 g, 2.0 mmol) dissolved in MeCN (50 mL), and the solution was stirred for 5 min. K_2PtCl_4 (0.84 g, 2.0 mmol) and DMSO (5 mL) were added to the reaction mixture, which was heated to 40 °C and stirred overnight. After cooling to room temperature, the solvent was removed under vacuum. A yellow precipitate was collected and dissolved in CH_2Cl_2 (10 mL). The organic layer was washed with water (3 × 10 mL), dried over Na_2SO_4, and concentrated to give a red solid (0.93 g, 71 %). ^{1}H NMR ($CDCl_3$, 300 MHz): δ = 8.33 (s, 2H), 7.70 (s, 2H), 7.25 (d, 2H), 7.05 (s, 2H), 6.53 (s, 2H), 6.22 (d, 2H), 3.40 (q, 8H), 1.23 ppm (t, 12H); ^{13}C NMR ($CDCl_3$, 300 MHz): δ = 167.2, 153.8, 145.6, 145.3, 136.6, 125.8, 114.8, 114.3, 105.5, 101.1, 45.1, 13.3 ppm; MS (FAB, +ve): *m/z*: 651 $[M]^+$; elemental analysis calcd (%) for $C_{28}H_{32}N_4O_2Pt$: C 51.61, H 4.95, N 8.60; found: C 51.60, H 4.91, N 8.51.

***N*,*N*′-Bis(4-diethylaminosalicylidene)-4,5-dichloro-1,2-phenylenediamine (H_2L^{1c})**: 4-(Diethylamino)salicylaldehyde (2 g, 10 mmol) in ethanol (10 mL) was added dropwise to 4,5-dichloro-*o*-phenylenediamine (0.92 g, 5.2 mmol) in ethanol (40 mL) at room temperature. The mixture was gradually heated to 60 °C and maintained at this temperature for 4 h. Upon removal of the solvent and cooling, a yellow precipitate was collected and recrystallized from ethanol to give the crude product (0.86 g, 35 %). ^{1}H NMR ($CDCl_3$, 300 MHz): δ = 13.43 (s, 2H), 8.33 (s, 2H), 7.24 (s, 2H), 7.12 (d, 2H), 6.20 (d, 2H), 6.15 (s, 2H), 3.39 (q, 8H), 1.21 ppm (t, 12H); ^{13}C NMR ($CDCl_3$, 300 MHz): δ = 164.9, 161.5, 152.7, 142.5, 134.5, 129.3, 120.7, 109.7, 104.5, 98.3, 45.1, 13.1 ppm; MS (FAB, +ve): *m/z*: 527 $[M]^+$.

[PtL^{1c}] (1c): Sodium acetate (0.11 g, 1.4 mmol) was added to H_2L^{1c} (0.36 g, 0.7 mmol) dissolved in MeCN (10 mL), and the solution was stirred for 5 min. K_2PtCl_4 (0.29 g, 0.7 mmol) and DMSO (1 mL) were added to the reaction mixture, which was heated to 40 °C and stirred overnight. After cooling to room temperature, the solvent was removed under vacuum. A yellow precipitate was collected and dissolved in CH_2Cl_2 (10 mL). The organic layer was washed with water (3×10 mL), dried over Na_2SO_4, and concentrated to give a red solid (0.22 g, 42.7%). ^{1}H NMR ($CDCl_3$, 300 MHz): δ = 8.25 (s, 2H), 7.85 (s, 2H), 7.29 (d, 2H), 6.54 (s, 2H), 6.29 (d, 2H), 3.39 (q, 8H), 1.23 ppm (t, 12H); MS (FAB, +ve): *m/z*: 720 $[M]^+$; elemental analysis calcd (%) for $C_{28}H_{30}Cl_2N_4O_2Pt$: C 46.67, H 4.20, N 7.78; found: C 46.60, H 4.21, N 7.71.

***N,N′*-Bis(4-diethylaminosalicylidene)-2,3-pyridylenediamine (H_2L^{1d})**: 4-(Diethylamino)salicylaldehyde (1 g, 5.2 mmol) in ethanol (5 mL) was added dropwise to 2,3-diaminopyridine (0.28 g, 2.6 mmol) in ethanol (5 mL) at room temperature. The reaction mixture was gradually heated to 60 °C and maintained at this temperature for 4 h. Upon removal of the solvent and cooling, a yellow precipitate was collected and recrystallized from ethanol to give the product (0.38 g, 32%). ^{1}H NMR ($CDCl_3$, 300 MHz): δ = 12.92 (s, 2H), 8.34 (s, 2H), 7.91 (d, 1H), 7.16–7.11 (m, 3H), 6.67 (m, 1H), 6.25~6.15 (m, 4H), 3.41 (q, 8H), 1.21 ppm (t, 12H); MS (FAB, +ve): *m/z*: 459 $[M]^+$.

[PtL^{1d}] (1d): Sodium acetate (0.16 g, 2.0 mmol) was added to H_2L^{1d} (0.43 g, 0.94 mmol) dissolved in MeCN (20 mL), and the solution was stirred for 5 min. K_2PtCl_4 (0.39 g, 0.94 mmol) and DMSO (2 mL) were added to the reaction mixture, which was heated to 40 °C and overnight. After cooling to room temperature, the solvent was removed under vacuum. A yellow precipitate was collected and dissolved in CH_2Cl_2 (10 mL). The organic layer was washed with water (3×10 mL), dried over Na_2SO_4, and concentrated to give a red solid (77.2 mg, 12.6%). ^{1}H NMR ($CDCl_3$, 300 MHz): δ = 9.19 (s, 1H), 8.40 (s, 1H), 8.23 (d, 1H), 8.07 (d, 1H), 7.44 (d, 1H), 7.28 (d, 1H), 7.06 (m, 1H), 6.57 (s, 2H), 6.30 (d, 2H), 3.42 (q, 8H), 1.23 ppm (t, 12H); MS (FAB, +ve): *m/z*: 653 $[M]^+$; elemental analysis calcd (%) for $C_{27}H_{31}N_5O_2Pt$: C 49.69, H 4.79, N 10.73; found: C 50.09, H 4.81, N 10.78.

***N,N′*-Bis(4-diethylaminosalicylidene)-1,2-ethylenediamine (H_2L^{2a})**: 4-(Diethylamino)salicylaldehyde (1 g, 5.2 mmol) in ethanol (5 mL) was added dropwise to 1,2-diaminoethane (0.16 g, 2.6 mmol) in ethanol (5 mL) at room temperature. The reaction mixture was gradually heated to 60 °C and maintained at this temperature for 4 h. Upon removal of the solvent and cooling, a yellow precipitate was collected and recrystallized from ethanol to give the product (0.86 g, 81%). ^{1}H NMR ($CDCl_3$, 300 MHz): δ = 12.72 (s, 2H), 8.02 (s, 2H), 6.95 (d, 2H), 6.13 (d, 2H), 6.09 (s, 2H), 3.76 (s, 4H), 3.34 (dd, 8H), 1.16 ppm (t, 12H); ^{13}C NMR ($CDCl_3$, 300 MHz): δ = 165.15, 164.76, 154.98, 133.37, 108.75, 103.46, 98.58, 58.66, 44.86, 13.12 ppm; MS (FAB, +ve): *m/z*: 411 $[M]^+$; elemental analysis calcd (%) for $C_{24}H_{34}N_4O_2$: C 70.21, H 8.35, N 13.65; found: C 69.99, H 8.34, N 13.52.

[PtL^{2a}] (2a): Sodium acetate (0.02 g, 0.24 mmol) was added to H_2L^{2a} (0.05 g, 0.12 mmol) dissolved in MeCN (10 mL), and the solution was stirred for 5 min. K_2PtCl_4 (0.05 g, 0.12 mmol) and DMSO (1 mL) were added to the reaction mixture, which was heated to 40 °C and stirred overnight. After cooling to room temperature, the solvent was removed under vacuum. A yellow precipitate was collected and dissolved in CH_2Cl_2 (10 mL). The organic layer was washed with water (3×10 mL), dried over Na_2SO_4, and concentrated to give a yellow solid (14 mg, 23%). ^{1}H NMR ($CDCl_3$, 300 MHz): δ = 7.75 (s, 2H), 7.07 (d, 2H), 6.46 (s, 2H), 6.09 (d, 2H), 3.64 (s, 4H), 3.33 (dd, 8H), 1.16 ppm (t, 12H); MS (FAB, +ve): *m/z*: 603 $[M]^+$; elemental analysis calcd (%) for $C_{24}H_{32}N_4O_2Pt$: C 47.76, H 5.34, N 9.28; found: C 47.67, H 5.38, N 9.31.

***N,N′*-Bis(4-diethylaminosalicylidene)-1,1,2,2-tetramethylethylenediamine (H_2L^{2b})**: 4-(Diethylamino)salicylaldehyde (0.51 g, 2.6 mmol) in ethanol (5 mL) was added dropwise to 2,3-diamino-2,3-dimethylbutane (0.16 g, 1.3 mmol) in ethanol (5 mL) at room temperature. The reaction mixture was gradually heated to 60 °C and maintained at this temperature for 4 h. Upon removal of the solvent and cooling, a yellow precipitate was collected and recrystallized from ethanol to give the product (0.34 g, 56%). ^{1}H NMR ($CDCl_3$, 300 MHz): δ = 7.93 (s, 2H), 6.92 (d 2H), 6.12 (d, 2H), 6.04 (s, 2H), 3.35 (dd, 8H), 1.39 (s, 12H), 1.16 ppm (t, 12H); ^{13}C NMR ($CDCl_3$, 300 MHz): δ = 169.81, 159.80, 152.67, 134.00, 108.65, 103.46, 99.41, 63.73, 44.89, 23.39, 13.18 ppm; MS (FAB, +ve): *m/z*: 467 $[M+1]^+$; elemental analysis calcd (%) for $C_{28}H_{42}N_4O_2$: C 72.07, H 9.07, N 12.01; found: C 71.37, H 9.08, N 11.81.

[PtL^{2b}] (2b): Sodium acetate (0.034 g, 0.42 mmol) was added to H_2L^{2b} (0.1 g, 0.21 mmol) dissolved in MeCN (10 mL), and the solution was stirred for 5 min. K_2PtCl_4 (0.085 g, 0.21 mmol) and DMSO (1 mL) were added to the reaction mixture, which was heated to 40 °C and stirred overnight. After cooling to room temperature, the solvent was removed under vacuum. A yellow precipitate was dissolved in CH_2Cl_2 (10 mL). The organic layer was washed with water (3×10 mL) dried over Na_2SO_4, and concentrated to give a yellow solid (84.2 mg, 61%). ^{1}H NMR ($CDCl_3$, 300 MHz): δ = 7.78 (s, 2H), 7.08 (d, 2H), 6.46 (s, 2H), 6.08 (d, 2H), 3.33 (dd, 8H), 1.41 (s, 12H), 1.17 ppm (t, 12H); ^{13}C NMR ($CDCl_3$, 300 MHz): δ = 165.46, 152.78, 149.54, 135.15, 114.03, 108.60, 104.73, 74.91, 44.92, 24.89, 13.21 ppm; MS (FAB, +ve): *m/z*: 659 $[M]^+$; elemental analysis calcd (%) for $C_{28}H_{40}N_4O_2Pt$: C 50.98, H 6.11, N 8.49; found: C 50.90, H 6.19, N 8.41.

General procedure for the synthesis of dendritic benzyl alcohols: A mixture of the appropriate dendritic benzyl bromide (2.00 equiv), 3,5-dihydroxybenzyl alcohol (1.00 equiv), dried potassium carbonate (2.50 equiv), and [18]crown-6 (0.2 equiv) in dry acetone was heated to reflux and stirred vigorously under nitrogen for 48 h. The reaction mixture was allowed to cool and evaporated to dryness under reduced pressure. The residue was partitioned between water and CH_2Cl_2 and the aqueous layer was extracted with CH_2Cl_2. The combined organic layers were dried and evaporated to dryness. The crude product was crystallized from ethyl acetate/hexane.

(Denron-G1)OH: Prepared from benzyl bromide (90%). ^{1}H NMR ($CDCl_3$, 300 MHz): δ = 7.34–7.43 (m, 10H), 6.68 (s, 2H), 6.62 (s, 1H), 5.04 (s, 4H), 4.62 ppm (d, 2H); MS (FAB, +ve): *m/z*: 320 $[M-1]^+$.

(Denron-G2)OH: Prepared from [Denron-G1]-Br (67.2%). ^{1}H NMR ($CDCl_3$, 300 MHz): δ = 7.33–7.42 (m, 20H), 6.68 (s, 4H), 6.60 (s, 2H), 6.59 (s, 2H), 6.56 (s, 1H), 5.03 (s, 8H), 4.97 (s, 4H), 4.6 ppm (d, 2H); MS (FAB, +ve): *m/z*: 745 $[M+1]^+$.

General procedure for the synthesis of dendritic benzyl bromides: Triphenylphosphine (1.25 equiv) was added to a mixture of the appropriate dendritic benzyl alcohol (1.00 equiv) and carbon tetrabromide (1.25 equiv) in dry THF, and the reaction mixture was stirred in a nitrogen atmosphere for 20 min. The reaction mixture was poured into water and extracted with CH_2Cl_2. The combined extracts were dried and evaporated to dryness. The crude product was crystallized from ethyl acetate/hexane.

(Denron-G1)Br: Prepared from [Denron-G1]-OH (89.2%). ^{1}H NMR ($CDCl_3$, 300 MHz): δ = 7.34–7.43 (m, 10H), 6.64 (s, 2H), 6.55 (s, 1H), 5.03 (s, 4H), 4.41 ppm (d, 2H); MS (FAB, +ve): *m/z*: 384 $[M]^+$.

(Denron-G2)Br: Prepared from [Denron-G2]-OH (75.1%). ^{1}H NMR ($CDCl_3$, 300 MHz): δ = 7.33–7.40 (m, 20H), 6.66 (s, 4H), 6.62 (s, 2H), 6.61 (s, 2H), 6.57 (s, 1H), 5.03 (s, 8H), 4.36 (s, 4H), 4.40 ppm (d, 2H); MS (FAB, +ve): *m/z*: 809 $[M+2]^+$.

(Denron-G1)salicylic aldehyde: K_2CO_3 (1.38 g, 0.01 mol) and KI (16.6 g, 0.1 mol) were added subsequently to a solution of 2,5-dihydroxybenzylaldehyde (1.38 g, 0.01 mol) and [Denron-G1]-Br (3.85 g, 0.01 mol) in acetone. The suspension was heated to reflux for 6 h. After cooling to room temperature, CH_2Cl_2, and H_2O were added, the layers were separated, and the aqueous layer was extracted. After drying over $MgSO_4$, the solvent was evaporated under vacuum and the resulting residue was purified by column chromatography (hexane/ethyl acetate = 3:1) to afford a yellow solid (1.33 g, 30%). ^{1}H NMR ($CDCl_3$, 300 MHz): δ = 7.31–7.42 (m, 10H), 7.19 (m, 2H), 6.84 (d, 1H), 6.65 (s, 2H), 6.57 (s, 1H), 5.03 (s, 4H), 4.93 ppm (s, 2H).

(Denron-G2)salicylic aldehyde: K_2CO_3 (0.15 g, 1.1 mmol) and KI (1.6 g, 0.01 mol) were subsequently added to a solution of 2,5-dihydroxybenzylaldehyde (0.15 g, 1.1 mmol) and [Denron-G2]-Br (0.88 g, 1.1 mmol) in acetone and the suspension was heated to reflux for 6 h. After cooling to room temperature, CH_2Cl_2 and H_2O were added, the layers were separated, and the aqueous layer was extracted. After drying over $MgSO_4$, the

solvent was evaporated under vacuum and the resulting residue was purified with column chromatography (hexane/ethyl acetate = 3:1) to afford a yellow solid (0.272 g, 63.1%). ^{1}H NMR ($CDCl_3$, 300 MHz): δ = 7.32–7.38 (m, 20H), 7.21 (m, 2H), 6.82 (d, 1H), 6.66 (s, 6H), 6.55 (s, 3H), 5.00 (s, 8H), 4.94 (s, 4H), 4.41 ppm (d, 2H).

***N,N′*-Bis[(G-1)dendritic salicylidene]-1,1,2,2-tetramethylethylenediamine] (H_2L^{2c})**: A solution of (G-1)dendritic salicylic aldehyde (0.6 g, 1.4 mmol) and 2,3-diamino-2,3-dimethylbutane (83 mg, 0.7 mmol) in ethanol (15 mL) was heated to reflux for 5 h. The solvent was evaporated and the residue was redissolved in diethyl ether. After the organic layer was washed with H_2O and brine and dried over $MgSO_4$, the solvent was evaporated and the residue was purified by column chromatography (hexane/CH_2Cl_2 = 2:1) to afford the product (0.24 g, 36%). ^{1}H NMR ($CDCl_3$, 300 MHz): δ = 8.30 (s, 2H), 7.33–7.40 (m, 20H), 7.21 (s, 2H), 6.96 (d, 2H), 6.88(s, 2H), 6.81(s, 4H), 6.57 (d, 2H), 5.03 (s, 8H), 4.97(s, 4H), 1.26 ppm (s, 12H); MS (FAB, +ve): *m/z*: 962 $[M+1]^+$; elemental analysis calcd (%) for $C_{62}H_{60}N_2O_8$: C 77.48, H 6.29, N 2.91; found: C 75.51, H 6.35, N 3.23.

[PtL^{2c}] (2c): K_2PtCl_4 (37 mg, 0.09 mmol) and NaOAc (15 mg, 0.18 mmol) were added to a solution of H_2L^{2c} (85.5 mg, 0.09 mmol) in MeCN (5 mL). DMSO (1 mL) was added to the reaction mixture, which was heated to 40°C and stirred overnight. The solvent was evaporated and the residue was dissolved in CH_2Cl_2 (10 mL). After the organic layer was washed with H_2O and brine and dried over $MgSO_4$, the solvent was evaporated and the residue was purified by column chromatography (hexane/CH_2Cl_2 = 1:1) to afford a yellow solid (14 mg, 13.6%). ^{1}H NMR ($CDCl_3$, 300 MHz): δ = 8.16 (s, 2H), 7.33–7.42 (m, 20H), 7.22 (s, 2H), 7.10 (d, 2H), 6.91(s, 2H), 6.75 (s, 4H), 6.60 (d, 2H), 5.03 (s, 8H,), 4.92 (s, 4H), 1.26 ppm (s, 12H); MS (FAB, +ve): *m/z*: 1152 $[M-1]^+$; elemental analysis calcd (%) for $C_{62}H_{58}N_2O_8Pt$: C 64.52, H 5.06, N 2.43; found: C 64.44, H 5.04, N 2.40.

***N,N′*-Bis[(G-2)dendritic salicylidene]-1,1,2,2-tetramethylethylenediamine] (H_2L^{2d})**: A solution of (G-2)dendritic salicylic aldehyde (0.28 g, 0.32 mol) and 2,3-diamino-2,3-dimethylbutane (20 mg, 0.16 mmol) in EtOH (5 mL) was heated to reflux for 5 h. The solvent was evaporated and the residue was dissolved in diethyl ether. After the organic layer was washed with H_2O and brine and dried over $MgSO_4$, the solvent was evaporated and the residue was purified by column chromatography (hexane/CH_2Cl_2 = 1:1) to afford the product (30 mg, 10.4%). ^{1}H NMR ($CDCl_3$, 300 MHz): δ = 8.20 (s, 2H), 7.26–7.38 (m, 40H), 7.08 (d, 2H), 6.68 (m, 4H), 6.66 (m, 10H), 6.56 (m, 8H), 5.01 (s, 16H), 4.96 (s, 8H), 4.63 (s, 4H), 1.25 ppm (s, 12H); MS (FAB, +ve): *m/z*: 1811 $[M+1]^+$; elemental analysis calcd (%) for $C_{118}H_{108}N_2O_{16}$: C 78.30, H 6.01, N 1.55; found: C 78.13, H 6.23, N 1.53.

[PtL^{2d}] (2d): K_2PtCl_4 (42 mg, 0.1 mmol) and NaOAc (16 mg, 0.2 mmol) were added to a solution of H_2L^{2d} (0.24 g, 0.1 mmol) in MeCN (5 mL). DMSO (1 mL) was added to the reaction mixture, which was heated to 40°C and stirred overnight. The solvent was evaporated and the residue was dissolved in CH_2Cl_2 (10 mL). After the organic layer was washed with H_2O and brine and dried over $MgSO_4$, the solvent was evaporated and the residue was purified by column chromatography (hexane/CH_2Cl_2 = 1:1) to afford a yellow product (83.2 mg, 32%). ^{1}H NMR ($CDCl_3$, 300 MHz): δ = 8.30 (s, 2H), 7.60–7.26 (m, 40H), 7.09 (d, 2H), 6.92 (s, 2H), 6.76 (m, 2H), 6.67 (m, 12H), 6.57 (m, 6H), 5.91 (m, 16H), 4.84 (s, 8H), 4.54 (s, 4H), 1.26 ppm (s, 12H); MS (FAB, +ve): *m/z*: 2002 $[M]^+$; elemental analysis calcd (%) for $C_{118}H_{106}N_2O_{16}Pt\cdot 2H_2O$: C 69.50, H 5.44, N 1.37; found: C 69.49, H 5.40, N 1.35.

***N,N′*-Bis{4-[1-(2-propylpiperidine)oxy]salicylidene}-4,5-methoxy-1,2-phenylenediamine (H_2L^3)**: 4-[1-(2-Propylpiperidine)oxy]salicylaldehyde (1 g, 4.0 mmol) in ethanol (5 mL) was added to 4,5-dimethoxy-*o*-phenylenediamine (0.34 g, 2.0 mmol) in ethanol (20 mL) at room temperature. The reaction mixture was gradually heated to 60°C and maintained at this temperature for 4 h. Upon removal of the solvent and cooling, a yellow precipitate was collected and recrystallized from ethanol to give the product (0.58 g, 46%). ^{1}H NMR ($CDCl_3$, 300 MHz): δ = 13.75 (s, 2H), 8.47 (s, 2H), 7.03 (d, 2H), 6.76 (s, 2H), 6.40–6.35 (m, 4H), 4.12 (t, 4H), 3.84 (d, 6H), 2.76 (t, 4H), 2.49 (t, 8H), 1.58 (m, 8H), 1.44 ppm (m, 4H); MS (FAB, +ve): *m/z*: 630 $[M]^+$.

[PtL^3] (3): Sodium acetate (0.02 g, 0.24 mmol) was added to H_2L^3 (0.15 g, 0.24 mmol) dissolved in MeCN (20 mL), and the solution was stirred for 5 min. K_2PtCl_4 (0.1 g, 0.24 mmol) and DMSO (1 mL) were added to the reaction mixture, which was heated to 40°C and stirred overnight. After cooling to room temperature, the solvent was removed under vacuum. A yellow precipitate was collected and dissolved in CH_2Cl_2 (10 mL). The organic layer was washed with water (3 × 10 mL), dried over Na_2SO_4, and concentrated to give a red solid (0.1 g, 51%). ^{1}H NMR ($CDCl_3$, 300 MHz): δ = 8.50 (s, 2H), 7.23 (d, 2H), 7.08 (s, 2H), 6.71 (s, 2H), 6.29 (d, 2H), 4.11 (t, 4H), 3.73 (s, 6H), 2.80 (t, 4H), 2.53 (t, 8H), 1.60 (m, 8H), 1.46 ppm (m, 4H); MS (FAB, +ve): *m/z*: 824 $[M]^+$; elemental analysis calcd (%) for $C_{36}H_{44}N_4O_6Pt$: C 52.48, H 5.38, N 6.80; found: C 52.44, H 5.38, N 6.78.

Polymerase stop assay: The polymerase stop assay was performed by using a modified protocol of the previously reported method.[19a] The reactions were performed in 1x PCR buffer, containing each pair of oligomers (G4A1 or G4A2; 10 μmol), deoxynucleotide triphosphate (dNTP; 0.16 mM), *Taq* polymerase (2.5 U), and increasing concentrations of the platinum(II) complex (from 1.25 to 50 μM). The reaction mixtures were incubated in a thermocycler under the following cycling conditions: 94°C for 3 min followed by 30 cycles of 94°C for 30 s, 58°C for 30 s, and 72°C for 30 s. The amplified products were resolved on 15% nondenaturing polyacrylamide gels in 1 × tris/borate/EDTA (TBE) buffer and silver stained.

NMR spectroscopic experiments: The NMR titration experiment was conducted in phosphate buffer (H_2O/D_2O (90:10) with KCl (150 mM), KH_2PO_4 (25 mM), and EDTA (1 mM); pH 7.0). G4A3-quadruplex DNA in buffer was titrated with a platinum(II) complex solution (10 μM in [D_6]DMSO). The spectra were recorded on 600-MHz Bruker spectrometers at 25°C.

Molecular modeling: A model study on the stacking interactions between **1a**/**3** and G-quadruplex DNA was performed by using Gaussian 03.[36] The platinum complex was optimized by using DFT calculations with a LanL2MB basis set.[35] The optimized structure of the platinum complex was used to do the docking. Molecular docking was performed by using the ICM-Pro 3.4–8a program (Molsoft).[30] According to the ICM method, the molecular system was described by using internal coordinates as variables. Energy calculations were based on the ECEPP/3 force field with a distance-dependent dielectric constant. The biased probability Monte Carlo (BPMC) minimization procedure was used for global-energy optimization. The BPMC global-energy-optimization method consists of 1) a random conformation change of the free variables according to a predefined continuous probability distribution; 2) local-energy minimization of analytical differentiable terms; 3) calculation of the complete energy including nondifferentiable terms such as entropy and solvation energy; 4) acceptance or rejection of the total energy based on the Metropolis criterion and return to step (1). The binding between **1a**/**3** and DNA was evaluated by binding energy, including grid energy, continuum electrostatic, and entropy terms. The initial models of loop isomers A and B were built from the X-ray crystal structures of human intramolecular telmoeric G quadruplex (PDB code: 1 KF1),[25] according to a previously reported procedure. Hydrogen and missing heavy atoms were added to the receptor structure followed by local minimization by using the conjugate gradient algorithm and analytical derivatives in the internal coordinates. In the docking analysis, the binding site was assigned across the entire structure of the DNA molecule. The ICM docking was performed to find the most favorable orientation. The resulting trajectories of the complex between **1a**/**3** and G-quadruplex DNA were energy minimized, and the interaction energies were computed.

Absorption titration: Solutions of the platinum(II) complexes (50 μM) were prepared in Tris/HCl buffer (10 mM; pH 7.4) containing KCl buffer (100 mM), and aliquots of a millimolar stock solution of G4A1 DNA in Tris/KCl buffer (0–500 μM) were added. Absorption spectra were recorded in the spectral range λ = 200–600 nm after equilibration at 20.0°C for 10 min.

Cell line: Human normal lung fibroblast (CCD-19Lu), human hepatocarcinoma (HepG2), human large-cell lung carcinoma (NCI-H460), and human cervical cancer (HeLa) were obtained from the American Type

Culture Collection (Rockville, MD). Human nasopharyngeal carcinoma cells (SUNE1) were generously provided by Prof. S.W. Tsao (Department of Anatomy, The University of Hong Kong). The cell cultures were maintained in RPMI-1640 medium supplemented with fetal bovine serum (10%), L-glutamine (1%), and *Penicillin streptomycin* (1%) in 25-cm^3 culture flasks at 37°C in a humidified atmosphere with 5% CO_2.

RNA extraction: Total RNA was extracted using the RNeasy mini kit. Briefly, 5×10^5 HepG2 cells were seeded in six-well plates and treated with the indicated concentrations of metal complexes after 24 h. The drug-treated and untreated cells were harvested after 24 h. The cell pellets were lysed and RNA was extracted according to the manufacturer's instruction and eluted in RNase-free water (50 μL).

RT-PCR: Reverse transcription was carried out by incubating RNA (1 μg), random primers (100 ng), and dNTPs (0.5 mM) at 65°C for 5 min, followed by a further incubation with SuperScript II Reverse Transcriptase (200 U) in 1×first-strand buffer at 42°C for 50 min. PCR amplifications were performed in a reaction containing cDNA (1 μL), dNTPs (200 μM), *Taq* DNA polymerase (2.5 U; Qiagen), 1×PCR buffer, and an aliquot of each primer (0.5 μM). PCR was performed for 22 cycles: 95°C for 15 s, 58°C for 30 s, and 72°C for 30 s. The samples were heated at 95°C for 5 min before the first cycle, and the extension time was lengthened to 5 min during the last cycle. The PCR products were size fractionated on a 1.3% agarose gel.

Cytotoxicity test (MTT Assay): The cells were seeded in a 96-well flat-bottomed microplate at 8000 cells $well^{-1}$ in growth medium solution (100 μL; fetal bovine serum (10%), L-glutamine (1%), and *Penicillin streptomycin* (1%) in RPMI-1640 medium or minimum essential medium). Each of the platinum(II) complexes and cisplatin (positive control) were dissolved in DMSO and mixed with the growth medium (final concentration: ≤1% DMSO). Serial dilution of each complex was added to each well. The microplate was incubated at 37°C in CO_2/air (95:5) in a humidified incubator for 48 h. After incubation, 3-(4,5-dimethylthiazol-2-yl)-2,5-diphenyl tetrasodium bromide (MTT) (10 μL, 5 mg mL^{-1}) was added to each well. The microplate was reincubated at 37°C in 5% CO_2 for 4 h. Solubilization solution (100 μL; sodium dodecyl sulphate (SDS; 10%) in HCl (0.01 M)) was added to each well. The microplate was left in an incubator for 24 h. The absorbance at $\lambda=580$ nm was measured by a microplate reader. The IC_{50} values of the platinum(II) complexes (the concentration that is required to reduce the absorbance by 50% relative to the controls) were determined by the dose dependence of the surviving cells after exposure to the metal complexes for 48 h.

Emission titration: Aliquots of a millimolar stock solution of G4A1 DNA in Tris/KCl buffer (0–1000 μM) were added to solutions of the platinum(II) complexes (50 μM) prepared in Tris/HCl (10 mM; pH 7.4) containing KCl buffer (100 mM). The emission spectra were recorded at $\lambda=$ 400–800 nm after equilibration at 20.0°C for 10 min.

Acknowledgements

This work was supported by the Area of Excellence Scheme established under the University Grants Committee (HKSAR, China (AoE/P-10/01), the University of Hong Kong (University Development Fund), and The Chinese Academy of Sciences—Croucher Foundation Funding Scheme For Joint Laboratories.

[1] S. Neidle, G. N. Parkinson, *Curr. Opin. Struct. Biol.* **2003**, *13*, 275.
[2] a) A. T. Phan, V. Kuryavyi, H. Y. Gaw, D. J. Patel, *Nat. Chem. Biol.* **2005**, *1*, 167; b) R. De Armond, S. Wood, D. Sun, L. H. Hurley, S. W. Ebbinghaus, *Biochemistry* **2005**, *44*, 16341; c) Y. Xu, H. Sugiyama, *Nucleic Acids Res.* **2006**, *34*, 949; d) J. Dai, T. S. Dexheimer, D. Chen, M. Carver, A. Ambrus, R. A. Jones, D. Yang, *J. Am. Chem. Soc.* **2006**, *128*, 1096; e) T. S. Dexheimer, D. Sun, L. H. Hurley, *J. Am. Chem. Soc.* **2006**, *128*, 5404.
[3] A. Siddiqui-Jain, C. L. Grand, D. J. Bearss, L. H. Hurley, *Proc. Natl. Acad. Sci. USA* **2002**, *99*, 11593.
[4] J. Dai, D. Chen, R. A. Jones, L. H. Hurley, D. Yang, *Nucleic Acids Res.* **2006**, *34*, 5133.
[5] D. Sun, K. Guo, J. J. Rusche, L. H. Hurley, *Nucleic Acids Res.* **2005**, *33*, 6070.
[6] S. Cogoi, L. E. Xodo, *Nucleic Acids Res.* **2006**, *34*, 2536.
[7] H. Fernando, A. P. Reszka, J. Huppert, S. Ladame, S. Rankin, A. R. Venkitaraman, S. Neidle, S. Balasubramanian, *Biochemistry* **2006**, *45*, 7854.
[8] S. Rankin, A. P. Reszka, J. Huppert, M. Zloh, G. N. Parkinson, A. K. Todd, S. Ladame, S. Balasubramanian, S. Neidle, *J. Am. Chem. Soc.* **2005**, *127*, 10584.
[9] a) C. A. Spencer, M. Groudine, *Adv. Cancer Res.* **1991**, *56*, 1; b) K. B. Marcu, S. A. Bossone, A. J. Patel, *Annu. Rev. Biochem.* **1992**, *61*, 809; c) L. M. Facchini, L. Z. Penn, *FASEB J.* **1998**, *12*, 633; d) S. Pelengaris, B. Rudolph, T. Littlewood, *Curr. Opin. Genet. Dev.* **2000**, *10*, 100; e) D. J. Patel, A. T. Phan, V. Kuryavyi, *Nucleic Acids Res.* **2007**, *35*, 7429.
[10] T. Simonsson, M. Pribylova and M. Vorlickova, *Biochem. Biophys. Res. Commun.* **2000**, *278*, 158.
[11] E. H. Postel, S. J. Berberich, J. W. Rooney, D. M. Kaetzel, *J. Bioenerg. Biomembr.* **2000**, *32*, 277.
[12] T. Simonsson, P. Pecinka, M. Kubista, *Nucleic Acids Res.* **1998**, *26*, 1167.
[13] E. F. Michelotti, T. Tomonaga, H. Krutzsch, D. Levens, *J. Biol. Chem.* **1995**, *270*, 9494.
[14] T. Tomonaga, D. Levens, *Proc. Natl. Acad. Sci. USA* **1996**, *93*, 5830.
[15] C. L. Grand, H. Han, R. M. Muñoz, S. Weitman, D. D. Von Hoff, L. H. Hurley, D. J. Bearss, *Mol. Cancer Ther.* **2002**, *1*, 565.
[16] J. Seenisamy, S. Bashyam, V. Gokhale, H. Vankayalapati, D. Sun, A. Siddiqui-Jain, N. Streiner, K. Shin-ya, E. White, W. D. Wilson, L. H. Hurley, *J. Am. Chem. Soc.* **2005**, *127*, 2944.
[17] A. Rangan, O. Y. Fedoroff, L. H. Hurley, *J. Biol. Chem.* **2001**, *276*, 4640.
[18] T. Lemarteleur, D. Gomez, R. Paterski, E. Mandine, P. Mailliet, J. F. Riou, *Biochem. Biophys. Res. Commun.* **2004**, *323*, 802.
[19] a) T.-M. Ou, Y.-J. Lu, C. Zhang, Z.-S. Huang, X.-D. Wang, J.-H. Tan, Y. Chen, D.-L. Ma, K.-Y. Wong, J. C.-O. Tang, A. S.-C. Chan, L.-Q. Gu, *J. Med. Chem.* **2007**, *50*, 1465; b) Y.-J. Lu, T.-M. Ou, J.-H. Tan, J.-Q. Hou, W.-Y. Shao, D. Peng, N. Sun, X.-D. Wang, W.-B. Wu, X.-Z. Bu, Z.-S. Huang, D.-L. Ma, K.-Y. Wong, L.-Q. Gu, *J. Med. Chem.* **2008**, *51*, 6381; c) Y. Ma, T.-M. Ou, J.-Q. Hou, Y.-J. Lu, J.-H. Tan, L.-Q. Gu, Z.-S. Huang, *Bioorg. Med. Chem.* **2008**, *16*, 7582.
[20] a) C. Orvig, M. J. Abrams, *Chem. Rev.* **1999**, *99*, 2201; b) B. Lippert, *Coord. Chem. Rev.* **1999**, *182*, 263; c) J. Reedijk, *Curr. Opin. Chem. Biol.* **1999**, *3*, 236; d) C. X. Zhang, S. J. Lippard, *Curr. Opin. Chem. Biol.* **2003**, *7*, 481; e) S. van Zutphen, J. Reedijk, *Coord. Chem. Rev.* **2005**, *249*, 2845; f) P. C. A. Bruijnincx, P. J. Sadler, *Curr. Opin. Chem. Biol.* **2008**, *12*, 197; g) R. W.-Y. Sun, C.-M. Che, *Coord. Chem. Rev.* **2009**, *253*, 1682.
[21] a) M. J. Abrams, B. A. Murrer, *Science* **1993**, *261*, 725; b) H.-L. Chan, D.-L. Ma, M. Yang, C.-M. Che, *ChemBioChem* **2003**, *4*, 62; c) H.-L. Chan, D.-L. Ma, M. Yang, C.-M. Che, *J. Biol. Inorg. Chem.* **2003**, *8*, 761; d) D.-L. Ma, C.-M. Che, *Chem. Eur. J.* **2003**, *9*, 6133; e) H. B. Gray, *Proc. Natl. Acad. Sci. USA* **2003**, *100*, 3563; f) S. J. Lippard, *Nat. Chem. Biol.* **2006**, *2*, 504; g) S. P. Fricker, *Dalton Trans.* **2007**, 4903; h) D.-L. Ma, C.-M. Che, F.-M. Siu, M. Yang, K.-Y. Wong, *Inorg. Chem.* **2007**, *46*, 740; i) R. W.-Y. Sun, D.-L. Ma, E. L.-M. Wong, C.-M. Che, *Dalton Trans.* **2007**, 4884.
[22] a) S. J. Lippard, *Acc. Chem. Res.* **1978**, *11*, 211; b) M. Howe-Grant, S. J. Lippard, *Biochemistry* **1979**, *18*, 5762; c) W. D. McFadyen, L. P. Wakelin, I. A. Roos, V. A. Leopold, *J. Med. Chem.* **1985**, *28*, 1113; d) G. Lowe, A. S. Droz, T. Vilaivan, G. W. Weaver, J. J. Park, J. M. Pratt, L. Tweedale, L. R. Kelland, *J. Med. Chem.* **1999**, *42*, 3167; e) G. Lowe, A. S. Droz, T. Vilaivan, G. W. Weaver, L. Tweedale, J. M. Pratt, P. Rock, V. Yardley, S. L. Croft, *J. Med. Chem.* **1999**, *42*, 999; f) J. A. Todd, L. M. Rendina, *Inorg. Chem.* **2002**, *41*, 3331; g) D.-L. Ma, T. Y.-T. Shum, F. Zhang, C.-M. Che, M. Yang, *Chem. Commun.* **2005**, 4675; h) M. L. Clark, R. L. Green, O. E. Johnson, P. E. Fanwick, D. R. McMillin, *Inorg. Chem.* **2008**, *47*, 9410.

[23] a) E. C. Long, J. K. Barton, *Acc. Chem. Res.* **1990**, *23*, 271; b) N. J. Turro, J. K. Barton, D. A. Tomalia, *Acc. Chem. Res.* **1991**, *24*, 332; c) K. E. Erkkila, D. T. Odom, J. K. Barton, *Chem. Rev.* **1999**, *99*, 2777.

[24] a) D.-F. Shi, R. T. Wheelhouse, D. Sun, L. H. Hurley, *J. Med. Chem.* **2001**, *44*, 4509; b) S. Redon, S. Bombard, M. A. Elizondo-Riojas, J. C. Chottard, *Biochemistry* **2001**, *40*, 8463; c) W. Tuntiwechapikul, M. Salazar, *Biochemistry* **2001**, *40*, 13652; d) I. V. Smirnov, F. W. Kotch, I. J. Pickering, J. T. Davis, R. H. Shafer, *Biochemistry* **2002**, *41*, 12133; e) J. E. Reed, A. A. Arnal, S. Neidle, R. Vilar, *J. Am. Chem. Soc.* **2006**, *128*, 5992; f) H. Bertrand, S. Bombard, D. Monchaud, M. P. Teulade-Fichou, *J. Biol. Inorg. Chem.* **2007**, *12*, 1003; g) S. E. Evans, M. A. Mendez, K. B. Turner, L. R. Keating, R. T. Grimes, S. Melchoir, V. A. Szalai, *J. Biol. Inorg. Chem.* **2007**, *12*, 1235; h) H. Bertrand, D. Monchaud, A. De Cian, R. Guillot, J. L. Mergny, M. P. Teulade-Fichou, *Org. Biomol. Chem.* **2007**, *5*, 2555; i) I. M. Dixon, F. Lopez, A. M. Tejera, J.-P. Estève, M. A. Blasco, G. Pratviel, B. Meunier, *J. Am. Chem. Soc.* **2007**, *129*, 1502; j) S. Shi, J. Liu, T. Yao, X. Geng, L. Jiang, Q. Yang, L. Cheng, L. Ji, *Inorg. Chem.* **2008**, *47*, 2910; k) R. Kieltyka, J. Fakhoury, N. Moitessier, H. F. Sleiman, *Chem. Eur. J.* **2008**, *14*, 1145; l) A. A. Arnal, J. B. Buchholz, S. Neidle, R. Vilar, *Inorg. Chem.* **2008**, *47*, 11910; m) D.-L. Ma, C.-M. Che, S.-C. Yan, *J. Am. Chem. Soc.* **2009**, *131*, 1835; n) J. E. Reed, A. J. P. White, S. Neidle, R. Vilar, *Dalton Trans.* **2009**, 2558.

[25] G. N. Parkinson, M. P. H. Lee, S. Neidle, *Nature* **2002**, *417*, 876.

[26] a) G. A. Shagisultanova, L. P. Ardasheva, *Russ. J. Coord. Chem.* **1999**, *25*, 788; b) C.-M. Che, S.-C. Chan, H.-F. Xiang, M. C.-W. Chan, Y. Liu, Y. Wang, *Chem. Commun.* **2004**, 1484; c) G. A. Shagisultanova, A. V. Shchukarev, T. V. Semenistaya, *Russ. J. Inorg. Chem.* **2005**, *50*, 912; d) L. P. Ardasheva, G. A. Shagisultanova, *Russ. J. Coord. Chem.* **2005**, *31*, 580; e) M. S. Masalovich, L. P. Ardasheva, G. A. Shagisultanava, *Russ. J. Appl. Chem.* **2007**, *80*, 1429; f) M. S. Masalovich, L. P. Ardasheva, G. A. Shagisultanova, *Russ. J. Appl. Chem.* **2007**, *80*, 2077.

[27] H. J. Kang, H. J. Park, *Biochemistry* **2009**, *48*, 7392.

[28] A. T. Phan, V. Kuryavyi, H. Y. Gaw, D. J. Patel, *Nat. Chem. Biol.* **2005**, *1*, 167.

[29] a) J. Seenisamy, E. M. Rezler, T. J. Powell, D. Tye, V. Gokhale, C. S. Joshi, A. Siddiqui-Jain, L. H. Hurley, *J. Am. Chem. Soc.* **2004**, *126*, 8702; b) A. T. Phan, Y. S. Modi, D. J. Patel, *J. Am. Chem. Soc.* **2004**, *126*, 8710.

[30] a) M. Totrov, R. Abagyan, *Proteins* **1997**, *29*, 215; b) D.-L. Ma, T.-S. Lai, F.-Y. Chan, W.-H. Chung, R. Abagyan, Y.-C. Leung, K.-Y. Wong, *ChemMedChem* **2008**, *3*, 881.

[31] C. V. Kumar, E. H. Asuncion, *J. Am. Chem. Soc.* **1993**, *115*, 8547.

[32] D. J. Welsh, S. P. Jones, D. K. Smith, *Angew. Chem.* **2009**, *121*, 4107; *Angew. Chem. Int. Ed.* **2009**, *48*, 4047.

[33] S. M. Haider, G. N. Parkinson, S. Neidle, *J. Mol. Biol.* **2003**, *326*, 117.

[34] M. A. Read, S. Neidle, *Biochemistry* **2000**, *39*, 13422.

[35] a) P. J. Hay, W. R. Wadt, *J. Chem. Phys.* **1985**, *82*, 270; b) W. R. Wadt, P. J. Hay, *J. Chem. Phys.* **1985**, *82*, 284; c) P. J. Hay, W. R. Wadt, *J. Chem. Phys.* **1985**, *82*, 299.

[36] Gaussian 03, Revision B.05, M. J. Frisch, G. W. Trucks, H. B. Schlegel, G. E. Scuseria, M. A. Robb, J. R. Cheeseman, J. A. Montgomery, Jr., T. Vreven, K. N. Kudin, J. C. Burant, J. M. Millam, S. S. Iyengar, J. Tomasi, V. Barone, B. Mennucci, M. Cossi, G. Scalmani, N. Rega, G. A. Petersson, H. Nakatsuji, M. Hada, M. Ehara, K. Toyota, R. Fukuda, J. Hasegawa, M. Ishida, T. Nakajima, Y. Honda, O. Kitao, H. Nakai, M. Klene, X. Li, J. E. Knox, H. P. Hratchian, J. B. Cross, V. Bakken, C. Adamo, J. Jaramillo, R. Gomperts, R. E. Stratmann, O. Yazyev, A. J. Austin, R. Cammi, C. Pomelli, J. W. Ochterski, P. Y. Ayala, K. Morokuma, G. A. Voth, P. Salvador, J. J. Dannenberg, V. G. Zakrzewski, S. Dapprich, A. D. Daniels, M. C. Strain, O. Farkas, D. K. Malick, A. D. Rabuck, K. Raghavachari, J. B. Foresman, J. V. Ortiz, Q. Cui, A. G. Baboul, S. Clifford, J. Cioslowski, B. B. Stefanov, G. Liu, A. Liashenko, P. Piskorz, I. Komaromi, R. L. Martin, D. J. Fox, T. Keith, M. A. Al-Laham, C. Y. Peng, A. Nanayakkara, M. Challacombe, P. M. W. Gill, B. Johnson, W. Chen, M. W. Wong, C. Gonzalez, J. A. Pople, Gaussian, Inc., Wallingford CT, **2004**.

Received: July 14, 2009
Published online: October 28, 2009

